DESIGN OF A SLIP OBSERVER AND ROAD ADHESION COEFFICIENT ESTIMATOR FOR ROAD VEHICLES

YOL ARAÇLARI İÇİN KAYMA GÖZLEMCİ VE YOL ADEZYON KATSAYISI TAHMINCISI TASARIMI

Arash HOSSEINIAN AHANGARNEJAD

Dr. S. Çağlar BAŞLAMIŞLI

Supervisor

Submitted to Institute of Graduate Studies in Science
of Hacettepe University as a partial fulfillment
to the requirements for the award of the degree of
MASTER OF SCIENCE
in
Mechanical Engineering

2013

This Study named "**Design of a Slip Observer and Road Adhesion Coefficient Estimator for Road Vehicles"** by **ARASH HOSSEINIAN AHANGARNEJAD** has been accepted as a thesis for the degree of **MASTER OF SCIENCE IN MECHANICAL ENGINEERING** by the below mentioned examining committee members.

Head

Dr. Özgür ÜNVER

Supervisor

Dr. S. Çağlar BAŞLAMIŞLI

Member

Assis. Prof. Dr. Ender CİĞEROĞLU

This thesis has been approved as a thesis for the degree of **MASTER OF SCIENCE IN MECHANICAL ENGINEERING** by the Board of Directors of the Instutute of Graduate Studies in Science of Hacettepe University.

Prof. Dr. Fatma SEVİN DÜZ

Director of the Institute of

Graduate Studies in Science

ETICES

In this thesis study, prepared in accordance with the spelling rules of Institute of Graduate Studies in Science of Hacettepe University,

I declare that

- all the information and documents have been obtained in the basis of the academic rules

- all audio-visual and written information and results have been presented according to the rules of scientific ethics

- in case of using other works, related studies have been cited in accorance with scientific standards

- all cited studies have been fully referenced

- I did not do any distortion in the data set

- and any part of this thesis has not been presented as another thesis study at this or any other university.

09 /04/ 2013

Arash HOSSEINIAN AHANGARNEJAD

DEDICATION

This dissertation is dedicated to my family especially to my father. This research could not have been possible without their love, support and patience. The many sacrifices they made to allow me to pursue this degree will be forever appreciated.

ABSTRACT

DESIGN OF A SLIP OBSERVER AND ROAD ADHESION COEFFICIENT ESTIMATOR FOR ROAD VEHICLES

Arash HOSSEINIAN AHANGARNEJAD

Master of Science, Mechanical Engineering

Supervisor: Dr. S. Çağlar BAŞLAMIŞLI

April 2013

Control systems that help the driver avoid accidents, or limit the damage in case of an accident, have become ubiquitous in modern passenger cars. For example, new cars typically have an anti-lock braking system (ABS), which prevents the wheels from locking during hard braking, and they often have an electronic stability control system (ESC), which stabilizes the lateral motion of the vehicle to prevent skidding. Collision warning and avoidance, rollover prevention, crosswind stabilization, and preparation for an impending accident by adjusting seat positions and seat belts are additional examples of control systems for automotive safety.

These systems rely on information about the state of the vehicle and its surroundings. To obtain this information, modern cars are equipped with various sensors. For a typical car with an ESC system, necessary measurements include the steering wheel angle, wheel angular velocities, lateral acceleration, and the rate of rotation around the vertical body-fixed axis, known as the yaw rate. These measurements alone contain a great deal of information about the state of the vehicle. The speed of the car

can be estimated using the wheel angular velocities, and a linear reference model taking the speed, steering wheel angle, and additional measurements as inputs can be used to predict the behavior of the car under normal driving conditions.

Although some quantities are easily measured, others are difficult to measure because of high cost or impracticality. When some quantity cannot be measured directly, it is often necessary to estimate it using the measurements that are available. Observers combine the available measurements with dynamic models to estimate unknown dynamic states.

Also, crucial parameters governing vehicle motion are the tire/road-surface coefficient of friction and tire model parameters. Vehicle stopping distance, safe following distance, safe speed, and lateral maneuverability all depend on this uncontrollable parameter.

Road friction and tire model parameters govern the tire forces, or forces that cause deceleration and traction and that prevent a vehicle from "spinning" during a panic maneuver. While other important parameters governing vehicle motion can be measured using transducers, there is currently no method to measure or otherwise determine road friction. In the absence of a "road fiction sensor", this project aims to estimate road friction and tire model parameters based on measured vehicle motion.

The numerical procedures developed in this project are based on extended Kalman filtering, a nonlinear adaptive filtering method. The adaptive tire requires a dynamic model of the vehicle and data that is gathered continually from sensors on board the vehicle. Ground vehicle motion depends largely on the tire forces, or forces that cause deceleration and traction and that can prevent a vehicle from losing lateral stability or "spinning" during severe maneuvers. The tire forces are nonlinear, and they depend on uncontrollable factors, such as tire/road-surface coefficient of friction (μ), tire model parameters, tire pressure and wear, and vehicle loads. While the latter parameters can be measured using standard sensors, there is currently no way to measure or otherwise determine μ and tire model parameters. In this project, the tire

forces, vehicle sideslip angle, longitudinal vehicle velocity and wheel slip are determined using extended Kalman filtering.

Özet

YOL ARAÇLARI İÇİN KAYMA GÖZLEMCİ VE YOL ADEZYON KATSAYISI TAHMINCISI TASARIMI

Arash HOSSEINIAN AHANGARNEJAD

Yüksek Lisans , Makina Mühendisliği

Tez Danışmanı: Dr. S. Çağlar BAŞLAMIŞLI

Nissan 2013

Sürücü kazaları önlemek, veya bir kaza halinde hasar sınırlamak yardımcı Kontrol sistemleri, modern yolcu arabaları her yerde olmuştur. Kontrol sistemleri, modern araclarda kazaların onlenmesine veya bir kaza halinde hasari sinirlamak icin surucuye yardimci olur. Örneğin, yeni bir araba genellikle sert frenleme sırasında tekerleklerin kilitlenmesini engelleyen bir anti-lock fren sistemi (ABS), var, ve genellikle önlemek için aracın yanal hareketini stabilize bir elektronik stabilite kontrol sistemi (ESC), var savrulma. Ornegin yeni araclarda sert frenleme esnasında tekerleklerin kilitlenmesini onleyen antilock fren sistemi ve aracin yanal hareketi sirasinda savrulmayi engelleyen elektronik stabilite kontrol sistemleri mevcuttur.Çarpışma uyarı ve kaçınma, rollover önleme, rüzgar stabilizasyonuna ve koltuk konumları ve emniyet kemerleri ayarlayarak yaklaşan bir kaza için hazırlık otomotiv güvenliği için kontrol sistemleri ek örnekler vardır. Carpisma uyari sistemi, ruzgar stabilizasyonu, koltuk konumlari ve emniyet kemerlerini ayarlayarak olasi bir kaza oncesi hazirlik gibi arac guvenligine yardimci ek ornekler de mevcuttur.

Bu sistemler aracın durumu ve çevresi hakkında bilgi güveniyor. Bu sistemler aracin

durumu ve etrafi hakkindaki bilgilere baglidir. Bu bilgileri almak için, modern otomobillerin çeşitli sensörler ile donatılmıştır.Modern otomobiller bu bilgileri elde edebilmek icin cesitli sensorlerle donatilmislardir. ESC sistemi ile tipik bir araç için gerekli ölçümleri yaw oranı olarak bilinen direksiyon açısı, tekerlek açısal hızlarda, yanal hızlanma ve dikey vücut sabit bir eksen etrafında dönme hızı, içerir. Tipik hir ESC li aracta gerekli olcumler "yaw" orani diye tabir edilen ve direksiyon acisi, tekerlek acsial hizlari, yanal ivmelenme ve dikey yonde sabit bir eksen etrafindaki donme hizindan olusmaktadir. Yalnız bu ölçümler aracın durumu hakkında bilgi büyük bir içerir. Sadece bu olcumler bile aracin durumu hakkinda cok onemli bilgiler icerir. Aracın hızı, tekerlek açısal hızlarının ve hız alarak doğrusal bir referans modeli kullanılarak simidi açısı, direksiyon ve girişleri gibi ek ölçümler normal sürüş koşullarında aracın davranışını tahmin etmek için kullanılabilecek tahmin edilebilir.Aracin hizi tekerleklerin acisal hziyla tahmin edilir ve dogrusal referans modeli aracin hizini direksiyon, simidi acisini ve bazi ek olcumleri alarak aracin normal surus sartlarindaki davranislarini tahmin eder.

Bazı miktarlarda kolaylıkla ölçülebilir olmasına rağmen, diğerleri yüksek olması nedeniyle maliyet veya impracticality ve ölçmek zordur. Bazi degerlerin kolaylikla olculebilmesine ragmen, bazilari yuksek maliyet ve ve pratik olmayislari sebebiyle zor olculur. Bir miktar doğrudan ölçülemez zaman, o zaman mevcut olan ölçümleri kullanılarak tahmin etmek genellikle gereklidir. Bazi degerlerin dogrudan olcumemesi sebebi ile diger olcumler kuallanilarak bu degerleri tahmin etmek gerekir. Gözlemciler bilinmeyen dinamik durumları tahmin etmek için dinamik modelleri ile kullanılabilir ölçümleri birleştirir.Gozlemciler dinamik modelleri kullanip olcumleri birlestirerek bilinmeyen dinamik durumlari tahmin edebilirler.

Ayrıca, araç hareket yöneten önemli parametreler lastik / sürtünme ve lastik model parametrelerinin yol yüzey katsayısı vardır. Ayrica arac hareket yonetiminde lastik-yol surtunme katsayisi ve lastik modeli gibi onemli parametreler vardır. Araç, güvenli bir hızda güvenli takip mesafesi, durma mesafesi ve lateral manevra tüm bu kontrol edilemeyen parametre bağlıdır. Guvenli takip mesafesi, durma mesafesi ve yatay manevra kabiliyeti gibi degerler tum bu kontrol edilemeyen degerler baglidir.

Yol sürtünme ve lastik model parametreleri yavaşlama ve çekiş neden ve bir panik manevra sırasında "iplik" bir araç önleyecek lastik güçleri veya kuvvetleri yönetir. Panikle yapilmis bir manevra sirasinda aracin spin atmasini onleyecek olan lastik kuvvetleri veya yavaslama ve cekis kuvvetlerini kontrol eder. Aracın hareket düzenleyen diğer önemli parametreleri dönüştürücüler kullanılarak ölçülebilir iken, ölçmek veya başka yol sürtünmesini tespit etmek için bir yöntem henüz yoktur. aracin hareketine etki eden diger parametreler olculebilirken, henuz yol surtunmesini olcebilecek herhangi bir yontem yoktur. Bir "yol kurgu sensörü" yokluğunda, bu proje ölçülen aracın hareket dayalı yol sürtünme ve lastik model parametrelerini tahmin etmeyi amaçlamaktadır.bu proje bir yol kurgu sensoru olmadan harekete dayali yol surtunmesini ve lastik model parametrelerini tahmin etmeyi amaclamaktadir.

Bu tezde geliştirilen sayısal işlemler genişletilmiş Kalman filtreleme, doğrusal olmayan adaptif filtreleme yöntemine dayanmaktadır. Uyarlamalı lastik tahta araç üzerinde sensörlerden gelen sürekli olarak toplanır ve taşıt verilerinin dinamik bir model gerektirir.adaptif lastik,aracin dinamik modeli ve arac uzerine yerlestirilmis olan sensorlerden alinan verilere ihtiyac duyar. Zemin Aracın hareket büyük ölçüde yavaşlama ve çekiş ve yanal kararlılık kaybetme veya şiddetli manevralar sırasında "iplik" bir araç önleyebilirsiniz neden lastik güçleri veya kuvvetleri bağlıdır. Aracin yuzeydeki hareketi lastik kuvvetleri veya yavaslamaya ve hizlanmaya sebep olan kuvvetlere baglidir ve ardarda manevralarda aracin yatay dengesini kaybetmesini engelleyecektir. Lastik kuvvetler doğrusal olmayan, ve onlar bu tür lastik / yol yüzeyi sürtünme katsayısı (μ), lastik model parametreleri, lastik basınç ve aşınma ve araç yükleri gibi kontrol edilemeyen faktörlere bağlıdır. Lastik kuvvetlerilineer degildir ve lastik-yol surtunmesi lastik model parametreleri lastik asinmasi, lastik basinci ve arac yukleri gibi parametrelere baglidir. Ikincilparametreleri standart sensörler kullanılarak ölçülebilir iken, ölçmek veya başka μ ve lastik model parametreleri belirlemek için bir yolu bulunmuyor. Ikincil parametreler standart sensorler kullanarak olculebiliyor iken μ ve lastik model parametrelerini belirlemek icin herhangi bir yol bulunmamaktadir. Bu projede, lastik güçleri, araç sideslip açısı, boyuna araç hızı ve tekerlek kayma oranı genişletilmiş Kalman filtresi kullanılarak belirlenmiştir.

ACKNOWLEDGMENTS

TABEL OF CONTENTS

LIST OF FIGURES

LIST OF TABLES

LIST OF SYMBOLS AND ABBREVIATIONS

Symbols

Quarter Car Model

B_x Magic Formula coefficient

C_x Magic Formula coefficient

c_i Burckhardt tire model parameters

D_x Magic Formula coefficient

E_x Magic Formula coefficient

J Inertia moment of wheel [kg m^2]: 1 [kg m^2]

v_x Longitudinal speed [m/s]

ω Wheel angular velocity [rad/s]

m Quarter car of mass [kg]: 450 [kg]

F_x Brake force in the wheel plane [N]

F_z Ground contact force [N]

W_r Tire radius [m]: 0.32 [m]

S_{vx} MagicFormula coefficient

T_b Braking torque [N.m]

μ_x Dynamic friction coefficient ($\frac{F_x}{F_z}$)

λ Wheel slip

λ^* Ideal wheel slip

Vehicle Dynamics

a_y Lateral acceleration [m/s^2]

B_y Magic Formula coefficient

c_i Rational tire model parameters

C_y Magic Formula coefficient

C_λ Longitudinal Cornering Stiffness

C_α Lateral Cornering Stiffness

D_y MagicFormula coefficient

E_y MagicFormula coefficient

F_{y_i} Tire cornering force [N]

F_{z_i} Vertical force [N]

g Gravitational acceleration [m/s^2]: 9.81 [m/s^2]

h_{CG} Height of CG [m] : 0.4 [m]

I_z Yaw moment of inertia [kg m^2]: 4510.25 [kg m^2]

l_f Distance from front axle to CG [m]: 1.1473 [m]

l_r Distance from rear axle to CG [m]: 1.48 [m]

m_v Vehicle mass [kg]: 1987.9 [kg]

r Yaw rate [rad/s]

S_{vy} Magic Formula coefficient

t Vehicle track [m]

v_x Longitudinal velocity [m/s]

v_y Lateral velocity [m/s]

μ Road friction coefficient

α_i Tire sideslip angle [rad]

β Vehicle body sideslip angle [rad]

δ Wheel steer angle [rad]

Kalman Filter

e_k Estimation error

f(x)   Non-linear system model

F(x)   System model jacobian

h(x)   Non-linear sensor model

H(x)   Output model jacobian

K   Optimal gain matrices

P_p Parameter error covariance

P_s State error covariance

R_p Measurement noise covariance matrices for parameter

R_s Measurement noise covariance matrices for state

Q_s Process noise covariance matrices for state

Q_p Process noise covariance matrices for parameter

Q_c Continuous process noise covariance matrices

S   Measurement/process noise cross covariance matrices

T_s Filter sampling interval [s]: 0.005[s]

x_s State vector

x_p Parameter vector

u   Input vector

v   Output noise

z_k Observation matrices

θ   Process noise

y   Output vector

κ   Moving average constant

τ   Moving average time constant for noise matrices memory

σ   Parameter error scaling factor

Abbreviations

ESC   Electronic Stability Control

EBD   Electronic Brakeforce Distribution

ABS   Anti-lock Braking System

DYC   Direct Yaw Moment Control

CG   Center of Gravity

KF   Kalman Filter

EKF   Extended Kalman Filter

1. INTRODUCTION

1.1. Motivation

Automobiles have become indispensable in our modern society. Consequently, vehicle safety has tremendous importance in our everyday lives. For some perspective, in the United States, motor vehicle crashes continue to be the leading cause of death for children, teens, and young adults. Worldwide, an estimated 1.2 million people are killed in road crashes each year and as many as 50 million are injured. Projections indicate that this will increase by about 65% over the next 20 years unless there is new commitment to prevention [1].

In order to prevent serious accidents, vehicle stability control such as ESC, EBD, ABS and DYC based on active safety technologies, has been widely applied to assist the driver to keep vehicle on the intended path. In order to design the ESC system, vehicle's actual behavior must be measured or estimated to be compared with the nominal behavior which is calculated from deriver's input [2]. The actual directional behavior of vehicle is calculated from motion variables, such as yaw rate, sideslip angle and road friction coefficient. Yaw rate is defined as the angular velocity of vehicle body around the vertical axis. Sideslip angle is defined as the angle between vehicle velocity vector at the center of gravity (CG) and the longitudinal axis. As seen in Figure 1.1, on a slippery road, yaw rate control can only maintain the vehicle in desired orientation, but the vehicle sideslip angle may increase significantly [3].

Experts estimate, for instance, that ESC prevents 27% of loss of control accidents and reduces single-vehicle crashes rates by 36% by intervening when emergency situations are detected [4], [5].
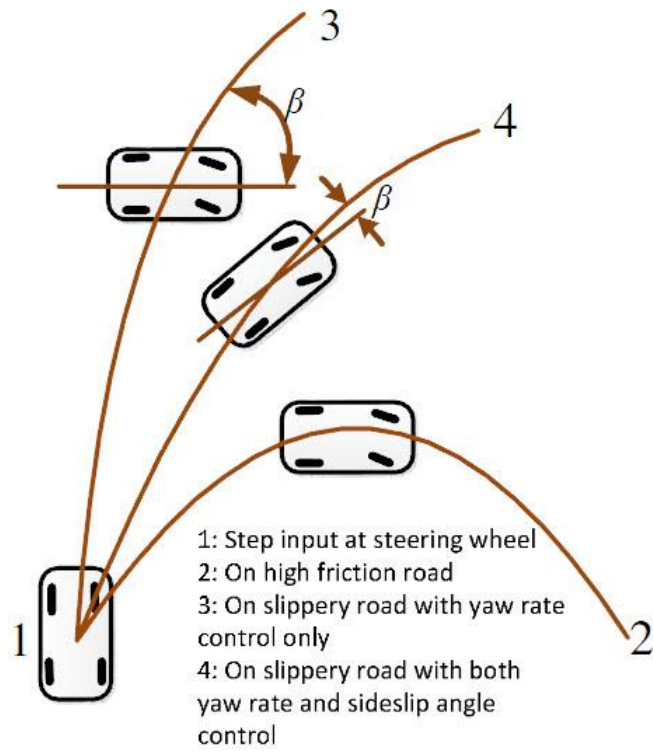
Figure 1.1 Vehicle motion with/without sideslip angle control [6]

While current vehicle safety systems such as ESC are unquestionably life-saving technologies, they are unfortunately limited by the lack of knowledge of the vehicle's state and operating conditions. Knowledge of the vehicle's sideslip angle is important information that is largely unavailable for current safety systems. The tire's lateral handling limits, which are the maximum potential grip a tire has on the road during a turn, are also generally unknown.

Overall, with improved knowledge of the vehicle's state and operating conditions, and with a coordinated approach to prevent unsafe vehicle trajectories, safety systems have an even greater potential to prevent vehicle accidents and reduce crash fatalities.

1.2. Background and Literature Review

A critical component of many modern vehicle control systems, such as stability control and lateral control system, requires the accurate knowledge of vehicle sideslip angle and yaw rate. The main function of the stability control system is to limit values of the vehicles yaw dynamics and sideslip angle to values that are

manageable to the driver. The yaw rate can be measured directly with a low-cost gyroscope. However the measurement of sideslip requires an expensive speed over ground sensor. Recently, it has been shown that Kalman filtering method was used to estimate unmeasurable states and unknown parameters.

Many methods have been proposed in the literature to estimate the latter states. A number of these methods have the basic limitation of using the classical automotive bicycle model which is only valid in the linear range of driving. Other proposed solutions do not incorporate adaptation schemes for the tire model, which is the major contribution of the present article. As a matter of fact, many different approaches for getting information about sideslip angle and road surface conditions have recently been analyzed. In order to estimate the slop of the friction force against the tire slip, a least-squares method in [7], is utilized on measurements of wheel angular velocity. Another least-square method for estimation of side slip angel and road friction was presented in [8]. A filtering scheme to estimate the maximum road-tire friction coefficient is consisted by an observer for lateral velocity in both [9] and [10], based primarily on utilizing the lateral acceleration measurement while a good measurement of the coefficient is necessary. In [11], by analyzing the ratio between slip values of the driven wheels and the normalized friction force, acquired using wheel angular velocities and engine torque, a Kalman filtering method is used so as to sort out conditions of the road surface. In [12], combining of an extended Kalman filter (EKF) with statistical methods for estimating the maximum road-tire friction coefficient is based on measurements of not only the yaw and roll rates, wheel angular velocities, and longitudinal and lateral accelerations, but also knowledge of the steering angle and total brake line pressure. The same procedure of EKF has been applied in [13] and [14]. In [15], based on measurements of wheel angular velocity, longitudinal tire slip, and wheel torque, they are applied both to adapt a friction parameter and to estimate of the wheel angular velocity. To estimate the longitudinal velocity, wheel angular velocity, and adaptation of a friction parameter, wheel angular velocity and torque is utilized in [16]. In both [15] and [16], convergence of the adapted friction parameters under conditions of nonzero longitudinal tire slip is analyzed. In [17] reduced-order observer is designed to estimate lateral velocity through applying a method for adaptation of the friction model to different road surface conditions. In

[18] and [19], the extended Kalman filter (EKF) method is suggested to be used to define the tire lateral force on the basis of a theoretical model and the results of experimental tests accomplished on the representing real model. In [20] two extended kalman filter in parallel are used to estimate states and parameters of vehicle.

1.3. Purpose of Thesis

The first purpose of this thesis is to estimate vehicle sideslip angle, road friction coefficient and tire model parameters in vehicle non-linear model. In this thesis, we set out to address three scenarios: estimation of sideslip angle, lateral velocity and front/rear axle cornering forces based on two measurements which are yaw rate and lateral acceleration where tire model parameters and road friction coefficient are unknown. Estimation of sideslip angle, lateral velocity and front/rear axle cornering forces based on two measurements which are yaw rate and lateral acceleration where tire model parameters and road friction coefficient are known. Estimation of sideslip angle, lateral velocity and tire forces based on measurement of yaw rate only where tire model parameters and road friction coefficient are known.

The second purpose of this thesis is estimation of sideslip angle based on measurement of yaw rate in linear vehicle model where sideslip angle is not large value.

The last purpose of the thesis is wheel slip regulation problem. Our aim is to estimate vehicle velocity, longitudinal tire slip, friction coefficient and tire model parameters in quarter car braking model.

1.4. Outline of Thesis

This dissertation is organized as follows: The explanation of various tire model, bicycle planer model, non-linear vehicle model and single wheel braking model in chapter 2. The theory of Kalman Filter and extended Kalman Filter is presented in chapter 3. Implementation of Kalman Filter and extended Kalman Filter algorithm to estimate vehicle sideslip angle, lateral velocity, tire cornering forces, rational tire model parameters and friction coefficient in chapter 4. Implementation of extended Kalman Filter algorithm to estimate wheel slip, vehicle velocity, friction coefficient

and Burckhardt tire model parameters in chapter 5. Finally, the conclusions are drawn in chapter 6.

2. VEHICLE DYNIMCS AND CONTROL

2.1. Introduction

This chapter covers the dynamics modeling of the vehicle, including various tire models, linear and non-linear planar vehicle model and quarter car braking model. Section 2.2 describes non-linear tire models (such as Pacejka magic formula, Burckhardt and rational tire models). Section 2.3 provides linear tire model. Section 2.4 shows the explanation of quarter car braking model. Section 2.5 covers the basic mathematical modeling of the vehicle's linear and non-linear vehicle dynamics. This non-linear vehicle model uses the non-linear tire model.

2.2. Non-linear Tire Model

Tire characteristics determine the dynamic behavior of the road vehicle. In this section, an introduction is given to the basic aspects of the force generating properties of the pneumatic tire. Pure slip characteristics of the tire are discussed and typical feature is presented.

The tires of a vehicle produce lateral forces as they deform with slip angles as shown in Figure 2.1. The slip angle, α, represents the angle between the tire's direction of travel and its contact patch and its longitudinal axis [21].

As the tire rolls, the tire contact patch over the ground deforms according to the direction of travel. This deformation and the elasticity of the tire produce lateral tire force [21]:

$$\alpha = \tan^{-1} \frac{v_y}{v_x} \tag{2.1}$$

For a freely rolling wheel, forward velocity v_x and angular speed of revolution ω can be obtained from measurements [23]. When a braking/tractive torque is applied about wheel spin axis, longitudinal slip arises. Longitudinal slip, λ, is defined as:

$$\lambda = \frac{v_x - W_r \omega}{v_x} \tag{2.2}$$
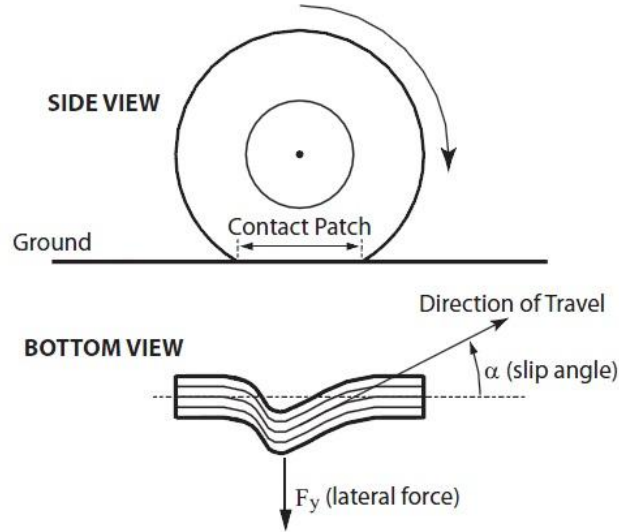
Figure 2.1. Rolling Tire Deformation and Lateral Force [22]

2.2.1. Pacejka Magic Formula

The Magic Formula [23] is an empirical tire modeling formulation widely used in vehicle dynamics studies. The Magic Formula empirically computes all tire force and moment components given tire sideslip angle, longitudinal slip, camber angle, normal load, and includes the effect of vehicle speed.

In case of pure longitudinal slip, tire longitudinal force can be obtained according to [23]:

$$F_{xo} = D_x \sin(C_x \arctan\{B_x(1 - E_x)(\lambda_x) + E_x \arctan[B_x(\lambda_x)]\}) + S_{vx} \qquad (2.3)$$

where $B_x, C_x, D_x, E_x, S_{vx}$ are coefficients which depend mainly on tire load F_z and tire camber angle which is neglected in this study. Their values are expressed as functions of a number of coefficients · κ and p which are characteristic of any specific tire. They are obtained from tire tests and do not have any direct meaning.

$$\lambda_x = \lambda + S_{Hx}$$

$$C_x = PC_{x1}\kappa_{Cx1}$$

$$D_x = \mu_x F_z$$

$$\mu_x = \frac{PD_{x1} + PD_{x2}df_z}{1 + \kappa_{\mu V}\lambda^V/v_0}\kappa_{\mu x}$$

$$E_x = (PE_{x1} + PE_{x2}df_z + PE_{x3}df_z^2)(1 - PE_{x4}\text{sign}(\lambda_x))\kappa_{E_x}$$

$$B_x = \frac{K_{x\lambda}}{C_x D_x + \varepsilon_x}$$

$$K_{x\lambda} = F_z(PK_{x1} + PK_{x2}df_z)\exp(PK_{x3}df_z)\kappa_{K_{x\lambda}}$$

$$S_{Hx} = (PH_{x1} + PH_{x1}df_z)\kappa_{H_x}$$

$$S_{Vx} = F_z(PV_{x1} + PV_{x2}df_z)\kappa_{V_x}\kappa'_{\mu x}$$

$$df_z = \frac{F_z - F_{z0}}{F_{z0}}$$

In case of pure sideslip, F_{y0} can be obtained according to

$$F_{yo} = D_y\sin\left(C_y\arctan\{B_y(1 - E_y)(\alpha_y) + E_y\arctan[B_y(\alpha_y)]\}\right) + S_{vy} \tag{2.4}$$

where

$$\alpha_s = \alpha^* + S_{Hx\,\alpha}$$

$$D_y = \mu_y F_z$$

$$E_x = (PE_{y1} + PE_{y2}df_z)(1 - PE_{y3}\text{sign}(\alpha_y))\kappa_{E_x}$$

$$C_y = PC_{y1}\kappa_{Cy}$$

$$\mu_y = \frac{PD_{y1} + PD_{y2}df_z}{1 + \kappa_{\mu V}\lambda\,{}^{V_s}/_{V_0}}\kappa_{\mu y}$$

$$B_y = \frac{K_{y\alpha}}{C_y D_y + \varepsilon_y}$$

$$K_{y\alpha} = PK_{y1}F'_{zo}\sin\left[2\arctan(\frac{F_z}{PK_{y2}F'_{zo}})\right]$$

$$B_y = \frac{K_{y\alpha}}{C_y D_y + \varepsilon_y}$$

$$S_{Hy} = (PH_{y1} + PH_{y1}df_z)\kappa_{H_y}$$

$$S_{Vy} = F_z(PV_{y1} + PV_{y2}df_z)\kappa_{V_y}\kappa'_{\mu y}$$

2.2.2. Burckhardt Tire Model

The friction behavior of the tires is shown in Figure 2.2. The friction co-efficient μ is defined as the ratio of the frictional force acting in the wheel plane F_x and the wheel ground contact force F_z:

$$\mu = \frac{F_x}{F_z} \tag{2.5}$$

The calculation of friction forces can be carried out using the method of Burckhardt [24]:

$$\mu = c_1\left(1 - e^{-c_2\lambda}\right) - c_3\lambda \tag{2.6}$$

Longitudinal and lateral force was expressed as:

$$F_x = F_z(c_1\left(1 - e^{-c_2\lambda}\right) - c_3\lambda) \tag{2.7}$$

$$F_y = F_z(c_1(1 - e^{-c_2\alpha}) - c_3\alpha) \tag{2.8}$$

The parameters c_1, c_2, and c_3 are given for various road surfaces in Table A.1 in Appendix.
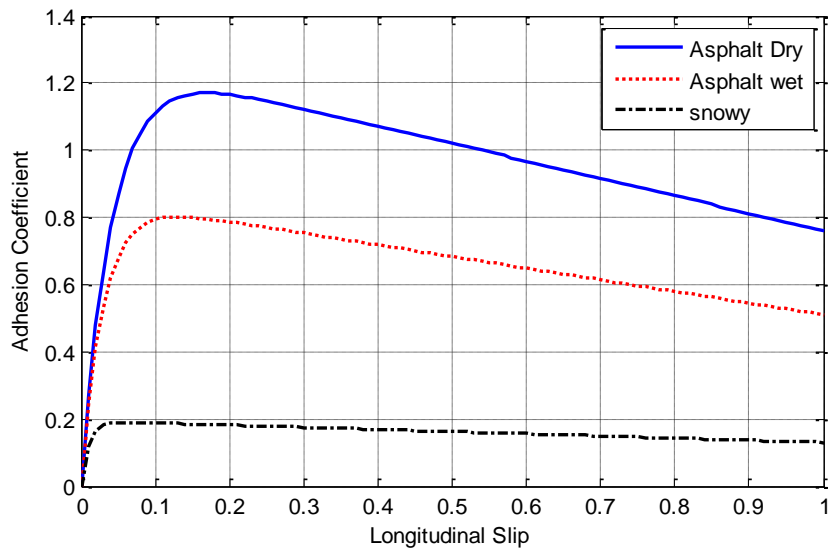
Figure 2.2. F_x predictions of Burckhardt tire model for various road adhesion coefficient, normal tire load of F_z=4kN and tire center speed v=20m/s

2.2.3. Rational Tire Model

Rational tire models have been used in the literature to provide a simple modeling alternative incorporating tire force features such as the dependence on normal load and road adhesion coefficient, the peaking behavior at a given slip and saturation and the dependence on both components of slip and dependence on tire center velocity [25].

Longitudinal and lateral force are expressed as:

$$F_x = c_2 \mu \frac{F_z}{F_{z0}} \left(\frac{\lambda c_1 (\mu + 1)}{(\lambda)^2 + c_1 (\mu + 1)} \right) \tag{2.9}$$

$$F_y = c_2 \mu \frac{F_z}{F_{z0}} \left(\frac{\alpha c_1 (\mu + 1)}{(\alpha)^2 + c_1 (\mu + 1)} \right) \tag{2.10}$$

where $c_1 (\mu + 1)$ has been introduced to cope with dependence of the peak locus of the cornering force on μ; c_1 and c_2 are constants [25]. In Figures 2.3, 2.4 and 2.5 comparison of F_x predictions of rational tire model, Magic Formula and Burckhardt tire model are shown.
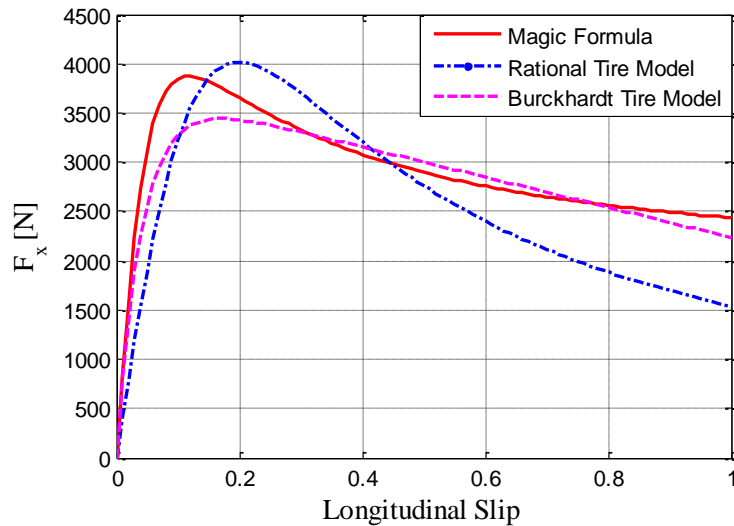
Figure 2.3. Comparison of F_x predictions of rational tire model, Burckhardt tire model and Magic Formula for road adhesion coefficient μ=1, normal tire load of F_z=4kN and tire center speed v=20m/s.
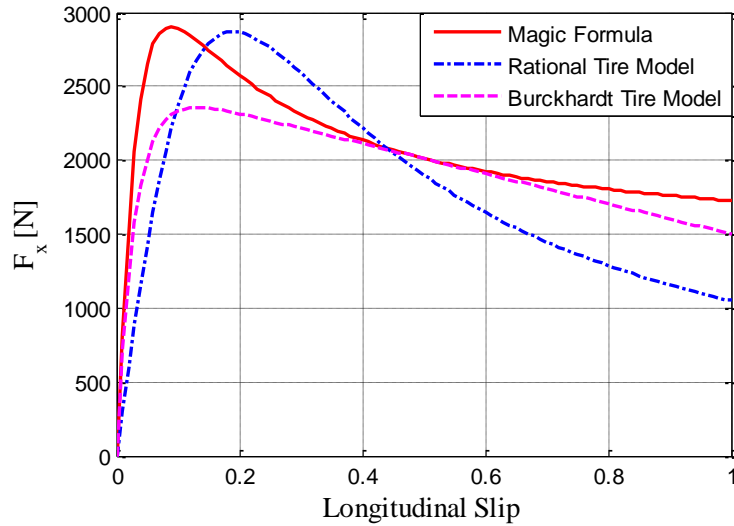
Figure 2.4. Comparison of F_x predictions of rational tire model, Burckhardt tire model and Magic Formula for road adhesion coefficient µ=0.6, normal tire load of F_z=4kN and tire center speed v=20m/s.
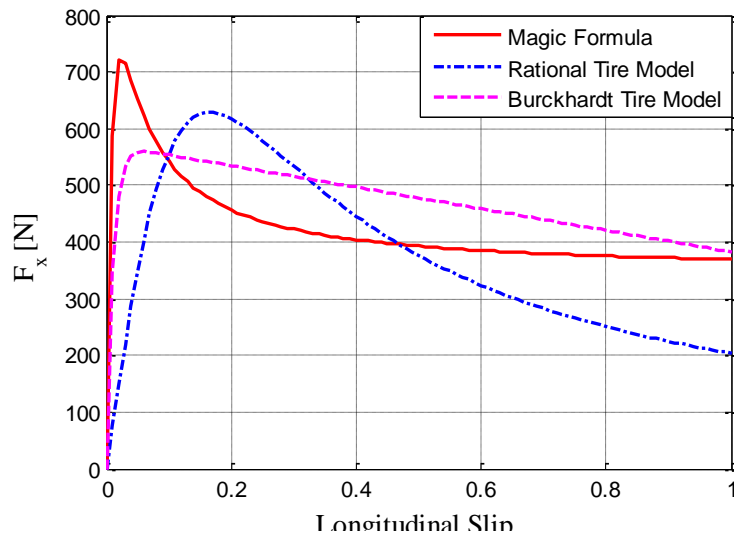
Figure 2.5. Comparison of F_x predictions of rational tire model, Burckhardt tire model and Magic Formula for road adhesion coefficient µ=0.3, normal tire load of F_z=4kN and tire center speed v=20m/s.

In Figures 2.6, 2.7 and 2.8 comparisons of F_y predictions of rational tire model, Burckhardt tire model and Magic Formula are shown.
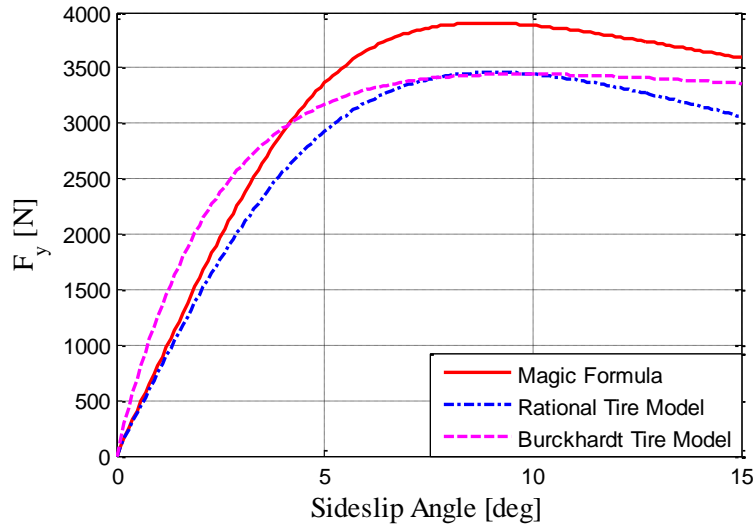
Figure 2.6. Comparison of F_y predictions of rational tire model, Burckhardt tire model and Magic Formula for road adhesion coefficient μ=1, normal tire load of F_z=4kN and tire center speed v=20m/s.
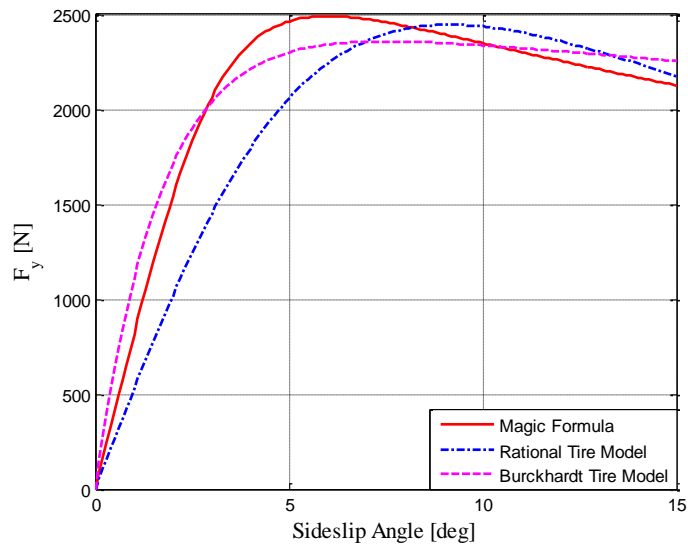
Figure 2.7. Comparison of F_y predictions of rational tire model, Burckhardt tire model and Magic Formula for road adhesion coefficient μ=0.6, normal tire load of F_z=4kN and tire center speed v=20m/s.
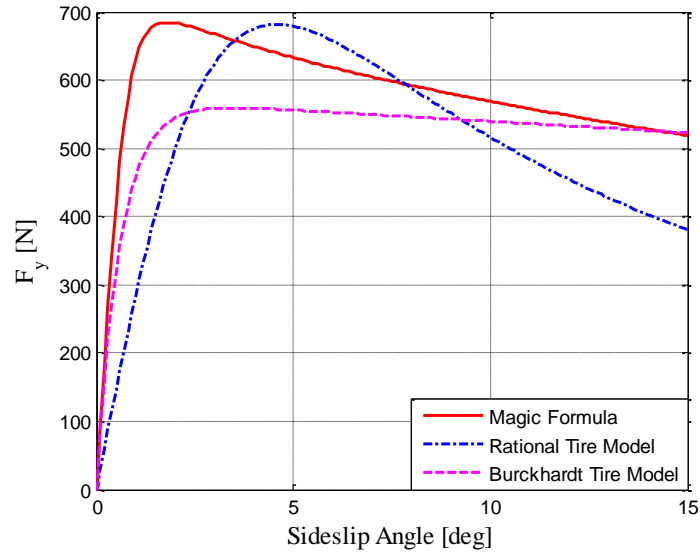
Figure 2.8. Comparison of F_y predictions of rational tire model, Burckhardt tire model and Magic Formula for road adhesion coefficient μ=0.3, normal tire load of F_z=4kN and tire center speed v=20m/s.

2.3. Linear Tire Model

This section explains fundamental concepts of linear tire model. In the linear region of the tire curve (small slip angle), the lateral force of the tire can be modeled as [3]:

$$F_y = C_\alpha \alpha \tag{2.11}$$

where cornering stiffness, C_α, represents the slope of initial portion of the tire curve [3]. The sign of α is taken such that the side force F_y is positive at positive sideslip angle. Figure 2.2 shows experimental measurements of the lateral force supplied by a tire as a function of the slip angle.
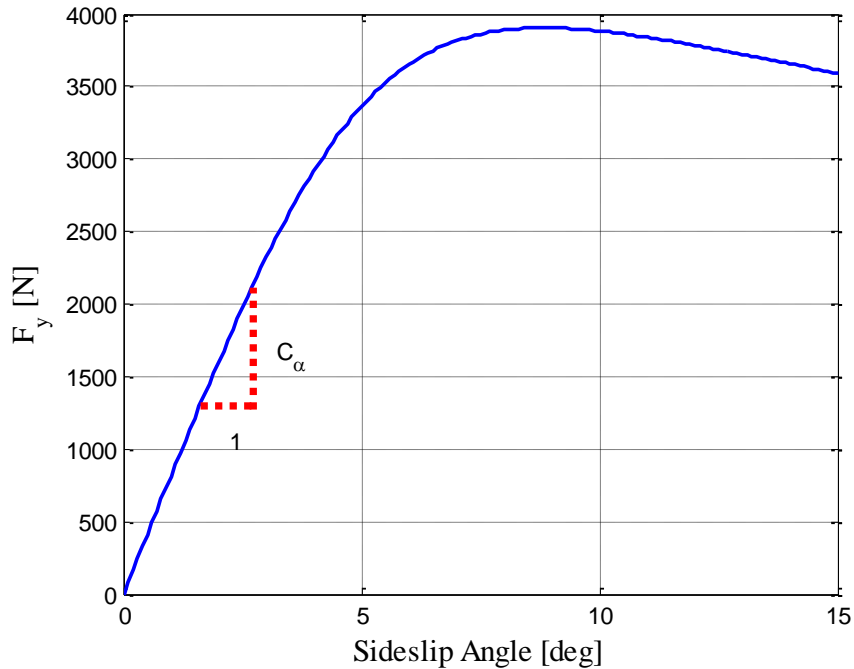
Figure 2.9. Tire lateral force and sideslip angle

The slopes of the pure slip curve at vanishing slip are defined as the longitudinal C_λ. Linearized force characteristics (valid at small levels of slip) can be represented by

$$F_x = C_\lambda \lambda \tag{2.12}$$

Its sign is taken such that, for a positive λ, a positive longitudinal force F_x arises.

2.4. single-Wheel Braking Model

In Figure 2.10 a model for the single wheel braking is shown. It comprises a mass of quarter car m, polar moment of inertia J, and tire radius W_r. It moves longitudinally with a speed v and rotational rate ω. Its weight mg is balanced by the reaction force Z, and the brake force F_x (sustained by the brake torque $T_b > 0$) decelerates the vehicle. The general equations for braking performance may be obtained from Newton's second Law written for the x-direction. Equations are given by [3]

$$J\dot{\omega} = W_r F_x - T_b \tag{2.13}$$

$$\dot{v}_x = \frac{1}{m} F_x \qquad (2.14)$$
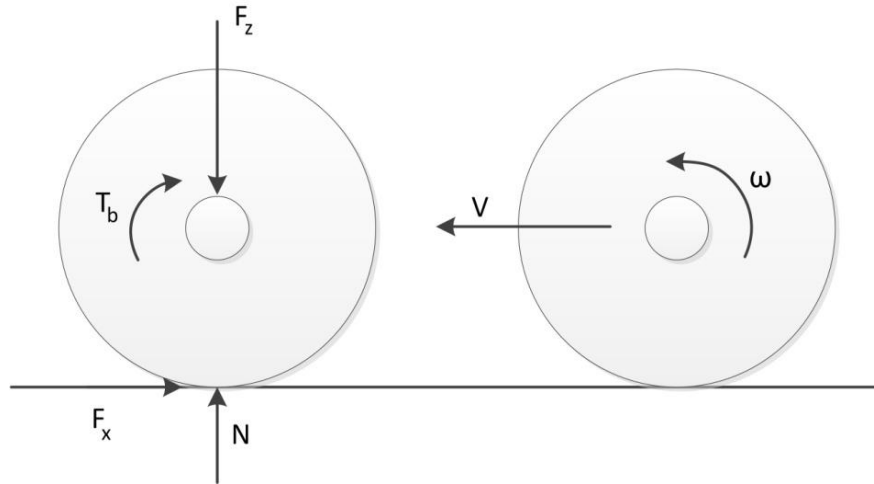
Figure 2.10. Schematic and free body diagram of the single-wheel braking model.

2.5. Planar Bicycle Model

The lateral dynamics of a vehicle in the horizontal plane are represented here by the single track, or bicycle model with states of lateral velocity, v_y, and yaw rate, r.

In Figure 2.11, δ is the steering angle, v_x and v_y are the longitudinal and lateral components of the vehicle velocity, $F_{y,f}$ and $F_{y,r}$ are the lateral tire forces, and α_f and α_r are the tire slip angles.

Derivation of the equations of motion for the bicycle model then follows from the following force and moment balances:

$$m_v a_y = F_{y,f} \cos\delta + F_{y,r} \qquad (2.15)$$

$$I_z \dot{r} = l_f F_{y,f} \cos\delta + F_{y,r} \qquad (2.16)$$

where I_z is the moment of inertia of the vehicle about its yaw axis, m_v is the vehicle mass, l_f and l_r are distance of the front and rear axles from the CG. The front and

rear tire forces, $F_{y,f}$ and $F_{y,r}$. The assumption that both the slip angle and the cornering stiffness are approximately the same for the inner and outer tires on each axle is inherent in this equation [26].

Linearized with the small angles, the tire slip angles, α_f and α_r, can be written in terms of v_x, v_y, r, and δ [26]:

$$\alpha_f \approx \delta - \frac{v_y + l_f r}{v_x} \tag{2.17}$$

$$\alpha_r \approx -\frac{v_y - l_r r}{v_x} \tag{2.18}$$

The state equation for the bicycle model can be then written as [26]:

$$\begin{bmatrix} \dot{\beta} \\ \dot{r} \end{bmatrix} = \begin{bmatrix} \dfrac{-C_{\alpha f} - C_{\alpha r}}{m_v v_x} & \dfrac{C_{\alpha r} l_r - C_{\alpha f} l_f}{m_v v_x^2} - 1 \\ \dfrac{C_{\alpha r} l_r - C_{\alpha f} l_f}{I_z} & \dfrac{-C_{\alpha f} l_f^2 - C_{\alpha r} l_r^2}{I_z v_x} \end{bmatrix} \begin{bmatrix} \beta \\ r \end{bmatrix} + \begin{bmatrix} \dfrac{C_{\alpha f}}{m_v v_x} \\ \dfrac{C_{\alpha f} l_f}{I_z} \end{bmatrix} \delta \tag{2.19}$$

Note that given the longitudinal and lateral velocities, v_x and v_y at any point on the vehicle body, the sideslip angle can be defined by:

$$\beta = tan^{-1}\left(\frac{v_y}{v_x}\right) \approx \frac{v_y}{v_x} \tag{2.20}$$
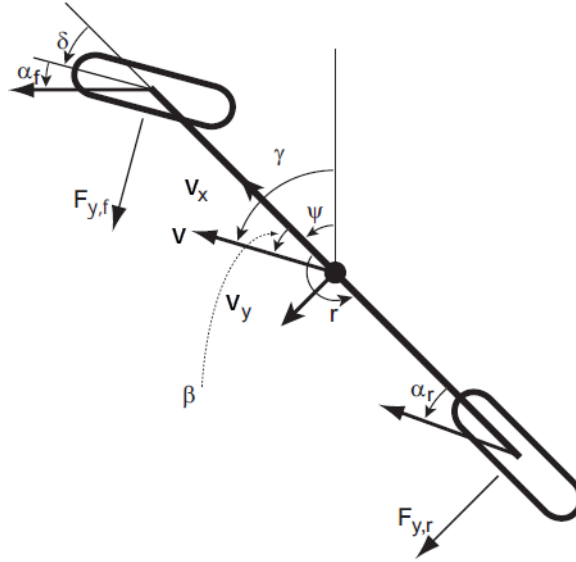
Figure 2.11. Bicycle Model [22]

2.6 Non-linear Planar Vehicle Modeling

The vehicle schematic shown in Figure 2.12 is a simple diagram of a four wheel vehicle in the lateral and longitudinal planes. In order to simplify the lateral dynamics, the longitudinal dynamics, including drive force and rolling resistance, were neglected. Additionally, the front and rear track widths (t) are assumed to be equal. As seen in Figure 2.12, the sideslip (β) of the vehicle is the difference between the velocity heading and the true heading of the vehicle. The yaw rate (r) is the angular velocity of the vehicle about the center of gravity. The lateral forces (F_y) are shown for both the inner and outer tires as well as the front and rear tires of the vehicle.

In Figure 2.12, the lateral dynamics of the vehicle are derived by summing the forces and the moments about the center of gravity of the vehicle as shown below [26].

$$\Sigma F_y = ma_y = \left(F_{y3} + F_{y4}\right) + \left(F_{y1} + F_{y2}\right)\cos\left(\delta\right) \tag{2.21}$$

$$\Sigma M_{cg} = I_z \dot{r} = -l_r\left(F_{y3} + F_{y4}\right) + l_f\left[\left(F_{y1} + F_{y2}\right)\cos(\delta)\right] + {}^t/_2\left[\left(F_{y1} + F_{y2}\right)\sin(\delta)\right] \tag{2.22}$$

17

Where

$$a_y = (vr + \dot{v}_y) = (vr + \dot{v}\sin(\beta) + v\dot{\beta}\cos(\beta)) \qquad (2.23)$$

By solving the above equations for β and $\dot{r}$, the equations of motion for thevehicles lateral dynamics can be found [26]

$$\dot{\beta} = \frac{(F_{y3} + F_{y4}) + (F_{y1} + F_{y2})\cos(\delta)}{m_{,,}v\cos(\beta)} - r - \frac{\dot{v}\tan(\beta)}{v} \qquad (2.24)$$

$$\dot{r} = \frac{-l_r(F_{y3} + F_{y4}) + l_f[(F_{y1} + F_{y2})\cos(\delta)] + \frac{t}{2}[(F_{y1} + F_{y2})\cos(\delta)]}{I_z} \qquad (2.25)$$
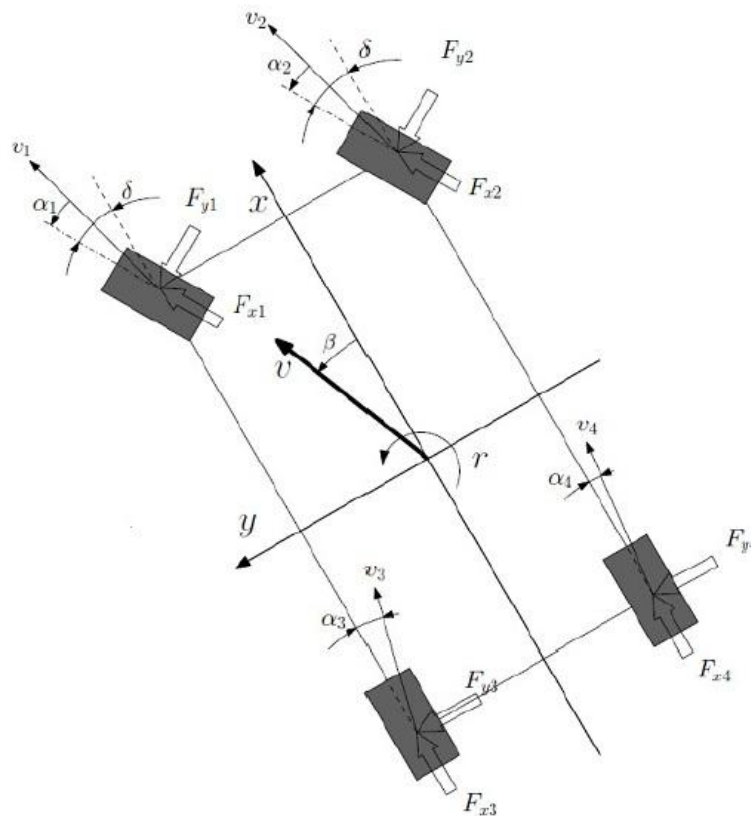
Figure 2.12. Four Wheel Vehicle Schematic Showing the Full Lateral Dynamics of a Vehicle [27]

The tire slip angle (α), as seen in Figure 2.12, is the difference between the tire's longitudinal axis and the tire's velocity vector. The tire velocity vector can be found by knowing the vehicle's velocity (at the center of gravity) and yaw rate. The direction or heading of the rear tire is the same as the vehicle heading, while the heading of the front tires must include the steer angle. The equation of the tire slip angles for all four tires is given as follows:

$$\alpha_1 = \delta - tan^{-1}\left(\frac{v\sin(\beta) + l_f r}{v\cos(\beta) - \frac{t}{2}r}\right) \tag{2.26}$$

$$\alpha_2 = \delta - tan^{-1}\left(\frac{v\sin(\beta) + l_f r}{v\cos(\beta) + \frac{t}{2}r}\right) \tag{2.27}$$

$$\alpha_3 = tan^{-1}\left(\frac{v\sin(\beta) - l_r r}{v\cos(\beta) - \frac{t}{2}r}\right) \tag{2.28}$$

$$\alpha_4 = tan^{-1}\left(\frac{v\sin(\beta) - l_r r}{v\cos(\beta) + \frac{t}{2}r}\right) \tag{2.29}$$

The vertical forces can be calculated as follows:

$$F_{z1,2} = \frac{l_r/2}{(l_f + l_r)}m_v g \pm m_v \frac{a_y h_{CG} l_r}{t(l_f + l_r)} \tag{2.30}$$

$$F_{z3,4} = \frac{l_f/2}{(l_f + l_r)}m_v g \pm m_v \frac{a_y h_{CG} l_f}{t(l_f + l_r)} \tag{2.31}$$

Where, l_f and l_r are the distances to the front axle and the rear axle; h_{CG} is the height of center of gravity.

3. KALMAN FILTER AND EXTENDED KALMAN FILTER

The Kalman Filter (KF) is a mathematical method used to use observed values containing noise and other disturbances and produce values closer to true value and calculate value. This filter has many applications basically in the vehicle, space and military technology.

The basic operation done by the KF is to estimate the true and calculated values, first by predicting a value, then calculating the uncertainty of the above value and finding an weighted average of both the predicted and measured values. Most weight is given to the value with least uncertainty. The result obtained the method gives estimates more closer to true values.

In order to use the KF the following should be provided: (1) knowledge of the system and measurement device dynamics, (2) the statistical description of the system noises, measurement errors and uncertainty in the dynamics models and (3) any available information about initial conditions of the variables of interest. The great advantage of KF from an implementation point of view is that it does not require all previous data to be kept in storage and reprocessed every time a new measurement is taken.

Although the KF assumes the system under consideration to be linear but this is not quite restricted. Its concept can be extended to some nonlinear applications as well. This will be discussed in later sections.

3.1. Discrete Time Kalman Filter

3.1.1 The process of estimation

The KF addresses the basic problem of estimation of the state of a discrete-time controlled process that is governed by the linear stochastic difference equation.

$$x_k = Fx_{k-1} + Bu_{k-1} + w_{k-1} \tag{3.1}$$

With a measurement:

$$z_k = Hx_k + v_k \tag{3.2}$$

The random variables in Eqs. 3.1 and 3.2 represent the process and measurement noise respectively. They are assumed to be independent of each other or in other

words they are uncorrelated. The noise is assumed to be white and with normal probability distributions. The process noise covariance matrix Q or measurement noise covariance matrix R may change with each time step or measurement, however we assume here they are constant matrices and in the difference equation which relates the states at previous time step to the state at current step [28].

3.1.2 The Computational Origins of the filter:

The $x_k^- \in R^n$ is defined as the a priori state estimate at time step k when the process prior to step k is known, and the a posteriori state estimate at step k when the measurement is known.

The a priori and a posteriori estimates errors can be defined as:

$$e_k = x_k - \hat{x}_k \tag{3.4}$$

The a priori estimate error covariance is then,

$$P_k^- = E[e_k^- e_k^{-T}] \tag{3.5}$$

The a posteriori estimate error covariance is,

$$P_k = E[e_k e_k^T] \tag{3.6}$$

The next step involves finding an equation that computes an a posteriori state estimate as a linear combination of an a priori estimate and a weighted difference between an actual measurement and a measurement prediction.

$$\hat{x}_k = \hat{x}_k^- + K(z_k - H\hat{x}_k^-) \tag{3.7}$$

The kalman gain calculated from the equation:

$$K_k = P_k^- H^T (H P_k^- H^T + R)^{-1} \tag{3.8}$$

The difference $(z_k - H\hat{x}_k^-)$ is the measurement innovation or residual. We see that as the R, measurement error covariance approaches zero, the gain K_k weights the residual more heavily [28].

3.1.3 Kalman Filtering Algorithm:

The Kalman Filter estimates a process by using a feedback control like form. The operation can be described as the process is estimated by the filter at some point of time and the feedback is obtained in the form of noisy measurements. The Kalman filter equations can be divided into two categories: time update equations and measurement update equations. To obtain the a priori estimates for the next time step the time update equations project forward (in time) the current state and error covariance estimates. The measurement update equations get the feedback to obtain an improved a posteriori estimate incorporating a new measurement into the a priori estimate.

3.1.4 Underlying Dynamic System Model:

KF is based on linear and non-linear dynamical systems discretized in the time domain. A vector of real numbers represents the state of the system. At each discrete time increment, a new state is generated applying a linear operator, with some noise added. Then, the observed states are generated using another linear operator with some added noise usually called as the measurement noise.

To use the KF to get estimations of the internal states of a process where only a sequence of noisy observations are known as inputs, the process is modeled in accordance with the state space representation of the Kalman filter. It means specifying the following matrices: the state transition model, the observation model, the covariance of the process noise, the covariance of the observation noise; and sometimes the control-input model for each time-step, $k, F_k, H_k, Q_k, P_k, B_k$, respectively as described further.

The KF model assumes the state at $(k-1)$ helps in measuring the true state at time k.

$$x_k = F_k x_{k-1} + B_k u_k + w_k \tag{3.9}$$

where F_k is the state transition state space model and it is applied to the previous state x_{k-1}; B_k is the control-input state space model and it is applied to the control vector u_k; w_k being the process noise and is drawn from a multivariate normal distribution with zero mean and covariance Q_k.

$$w_k \sim N(0, \ Q_k) \tag{3.10}$$

An observation z_k of the true state x_k time k is made according to

$$z_k = Hx_k + v_k \tag{3.11}$$

Here H_k is the observation state space model which helps in mapping the observed space from true space and v_k is the observation or measurement noise (Gaussian white noise) with zero mean and covariance R_k.

$$v_k \sim N(0, \ R_k) \tag{3.12}$$

Starting from the initial states to the noise vectors at each step are mutually independent.

A lot of real dynamical systems do not exactly fit this model as the KF mainly deals with linear systems and almost all real systems are non-linear. In fact, unmodelled dynamics can reduce the filter performance, though it is supposed to work finely with inputs which are unknown stochastic signals. The estimation algorithm can become unstable because the effect of unmodelled dynamics is dependent on the inputs. But the use of white Gaussian noise will not make the algorithm diverge and so in the thesis the noise used as input noise and measurement noise are Gaussian white noise [28].

3.1.5 Mathematical Formulation in steps:

The KF is a recursive estimator. Only the estimated state from the previous time step and the current measurement are required to compute the estimate for the current state.

The notation $\hat{x}_{n|m}$ shows the estimate x of at time n, when observations till time m is obtained.

The two variables that can represent the filter:

- $\hat{x}_{k|k}$, the a posteriori state estimate at time k
- $P_{k|k}$, the a posteriori error covariance matrix (a measure of the estimated accuracy of the state estimate).

Predict

Predicted (a priori) state

$$\hat{x}_{k|k-1} = F_k\hat{x}_{k-1|k-1} + B_ku_k \tag{3.13}$$

Predicted (a priori) estimate covariance

$$P_{k|k-1} = F_kP_{k-1|k-1}F_k^T + Q_k \tag{3.14}$$

Update

Innovation or measurement residual

$$\hat{y}_k = z_k - H_k\hat{x}_{k|k-1} \tag{3.15}$$

Innovation (or residual) covariance

$$S_k = H_kP_{k|k-1}H_k^T + R_k \tag{3.16}$$

Optimal Kalman gain

$$K_k = P_{k|k-1}H_k^TS_k^{-1} \tag{3.17}$$

Updated (a posteriori) state estimate

$$\hat{x}_{k|k} = \hat{x}_{k|k-1} + K_k\hat{y}_k \tag{3.18}$$

Updated (a posteriori) estimate covariance

$$P_{k|k} = (I - K_kH_k)P_{k|k-1} \tag{3.19}$$

3.2. Continuous Time Kalman Filter

Kalman and Bucy presented continuous-time version of the Kalman filter [29] one year after Kalman's work on the optimal filtering. For this reason, the continuous time filter is sometimes called the Kalman-Bucy filter. The Kalman filter applications are implemented in digital computers, therefore, the continuous time Kalman filter has been used more for theory than practice. Consider a linear system in which the state x(t) and measurements y(t) satisfy

$$\dot{x}(t) = A_c x(t) + Bu(t) + Gw(t) \tag{3.20}$$

$$y(t) = Hx(t) + v(t) \tag{3.21}$$

$\dot{x}(t)$ denotes the derivative of the state $x(t)$ and G is the process noise to state matices. We assume that process noise $w(t)$ and measurement noise $v(t)$ are uncorrelated Gaussian stationary white noise with zero mean, namely

$$E\big(w(t)\big) = 0 \tag{3.22}$$

$$E\big(v(t)\big) = 0 \tag{3.23}$$

and

$$E(w(t)w(\tau)^T) = Q_c\delta(t - \tau) \tag{3.24}$$

$$E(v(t)v(\tau)^T) = R\delta(t - \tau) \tag{3.25}$$

$\delta(t - \tau)$ is the delta dirac function, which has a value of ∞ at $t = \tau$, a value of 0 everywhere else. We note that, discrete-time white noise with covariance Q in a system with a sample period of Δt, is equivalent to continuous-time white noise with covariance $Q_c = Q/\Delta t$, [30]. The continuous-time Kalman filter has the form:

$$\dot{\hat{x}}(t) = A_c\hat{x}(t) + Bu(t) + K(t)(y(t) - H\hat{x}(t)) \tag{3.26}$$

where the Kalman gain k(t) is

$$K(t) = P(t)H^T R^{-1} \tag{3.27}$$

and the state error covariance matrix $P(t)$ satisfies

$$\dot{P}(t) = A_c P(t) + P(t){A_c}^T - P(t)H^T R^{-1}HP(t) + GQ_cG^T \tag{3.28}$$

which is called a differential algebraic Riccati equation. By letting $t \to \infty$ such that $\dot{P}(t) = 0$, a steady state solution for P(t), which we denote as P, is obtained from

$$0 = A_c P + P H^T R^{-1} H P + G Q_c G^T \tag{3.29}$$

The expressions given in Eqs. 3.26, 3.27 and 3.28 constitute the continuous-time Kalman filter. The distinction between the prediction and update steps of discrete-time Kalman filtering does not exist in continuous time and the covariance of the innovation process $(e(t) = y(t) - H\hat{x}(t))$ is equal to the covariance of measurement noise R, namely

$$E(e(t)e(\tau)^T) = R\delta(t - \tau) \tag{3.30}$$

3.3. Extended Kalman Filter:

It is known that the real systems that are inspiration for all these estimators like Kalman Filter are governed by non-linear functions. So we always need the advanced version of the Filters that are basically designed for linear filters. Similarly it is said that in estimation theory, the extended Kalman filter (EKF) is the nonlinear version of the Kalman filter. This non-linear filter linearizes about the current mean and covariance [28].

3.3.1. Formulation:

In the EKF, the state transition and observation state space models may not be linear functions of the state but might be many non-linear functions.

$$x_k = f(x_{k-1}, u_{k-1}) + w_{k-1} \tag{3.31}$$

$$z_k = h(x_k) + v_k \tag{3.32}$$

Where w_k and v_k are the process and observation noises which are both assumed to be zero mean multivariate Gaussian noise with covariance Q_k and R_k respectively.

The functions f and h use the previous estimate and help in computing the predicted state and again the predicted state is used to calculate the predicted

measurement. However, f and h cannot be used to the covariance directly. So a matrix of partial derivatives (the Jacobian) computation is required.

At each time step with the help of current predicted states the Jacobian is calculated. These matrices are used in the KF equations. This process actually linearizes the non-linear function around the present estimate.

3.3.2. Predict and Update Equations:

Predict

Predicted state

$$\hat{x}_{k|k-1} = f(\hat{x}_{k-1|k-1}, u_{k-1}) \tag{3.33}$$

Predicted estimate covariance

$$P_{k|k-1} = F_{k-1}P_{k-1|k-1}F_{k-1}^T + Q_{k-1} \tag{3.34}$$

Update

Innovation or measurement residual

$$\hat{y}_k = z_k - h(\hat{x}_{k|k-1}) \tag{3.35}$$

Innovation (or residual) covariance

$$S_k = H_k P_{k|k-1} H_k^T + R_k \tag{3.36}$$

Optimal Kalman gain

$$K_k = P_{k|k-1} H_k^T S_k^{-1} \tag{3.37}$$

Updated state estimate

$$\hat{x}_{k|k} = \hat{x}_{k|k-1} + K_k \hat{y}_k \tag{3.38}$$

Updated estimate covariance

$$P_{k|k} = (I - K_k H_k)P_{k|k-1} \tag{3.39}$$

where the state transition and observation matrices are defined to be the following Jacobians:

$$F_{k-1} = \frac{\partial f}{\partial x}\Big|_{\hat{x}_{k-1|k-1}, u_{k-1}} \tag{2.40}$$

$$H_k = \frac{\partial h}{\partial x}\Big|_{\hat{x}_{k|k-1}} \tag{2.41}$$

Another important point to be noted is that the performance of all the estimators given above may not be optimized since covariances, Q_0, R_0, P_0 are tuned by trial and error. Nevertheless it is evident that the algorithms should give reasonable results when the system is well tuned.

3.3.3 Limitations of EKF:

Even though the EKF is most commonly used to approximate a solution for nonlinear estimation and filtering, it suffers some serious limitations [28].

1. Linearized transformations are only reliable if the error propagation can be well approximated by a linear function. In the situation where the condition does not hold, the linearization can be extremely poor. This might have the slight effect of degrading the filter performance or as a serious effect as causing the filter to divert.

2. Linearization can be applied only if the jacobian matrix exists. Unfortunately, this is not always the case. For example if the system possesses discontinuities, in which the parameters can change abruptly, or have singularities, the Jacobian matrix does not exist and linearization can not be done.

3. Calculating the Jacobian matrices can be a very difficult and error-prone process. For a higher order system this involves a dense algebraic effort and possibly leads to errors.

4. By using a simple "first order Taylor series linearization", the algorithm neglects the fact that the prior and predicted state variables, i.e. $\hat{x}^+(k-1)$ and $\hat{x}^-(k)$ are in fact the random variables. This can seriously affect the accuracy of the posterior predictions and hence the final state estimates generated by the filter. Since it fails

to generate consistent estimates of the estimation error covariance it causes the filter to "trust" its own estimates more than is warranted by the true underlying state-space evolution and observation sequences.

3.4 Dual Extended Kalman Filter

One important application of the Extended Kamlan Filter (EKF) is parameter or coefficient identification in linear or nonlinear systems. Here it should be noted that no matter whether the system is linear or nonlinear, only the EKF can be applied for parameter identification. In many applications, it is necessary to estimate parameters and coefficients which are impossible to measure or to be known. The EKF provides an effective approach in estimating such parameters.

This approach has also been developed for joint state/parameter estimation under the name Dual Extended Kalman Filter (DEKF) as first proposed by Wan and Nelson [28]. In this method, two EKFs are used in parallel for combined state and parameter estimation.

In the dual filtering approach, a separate state-space representation is used for the states and the parameters. Thus two estimators are run simultaneously for state and parameter estimation as shown in Figure 3.1.

In general a non-linear system can be formulated as:

$$x_s(t+1) = f\left(x_s(t), u(t), x_p(t), w(t)\right) \tag{3.42}$$

$$y(t) = h(x_s(t), v(t), x_p(t)) \tag{3.43}$$

where x_s is the state vector, x_p is the parameter vector, u is the input vector, y is the output vector, with w and v being the process noise and output noise vectors respectively.
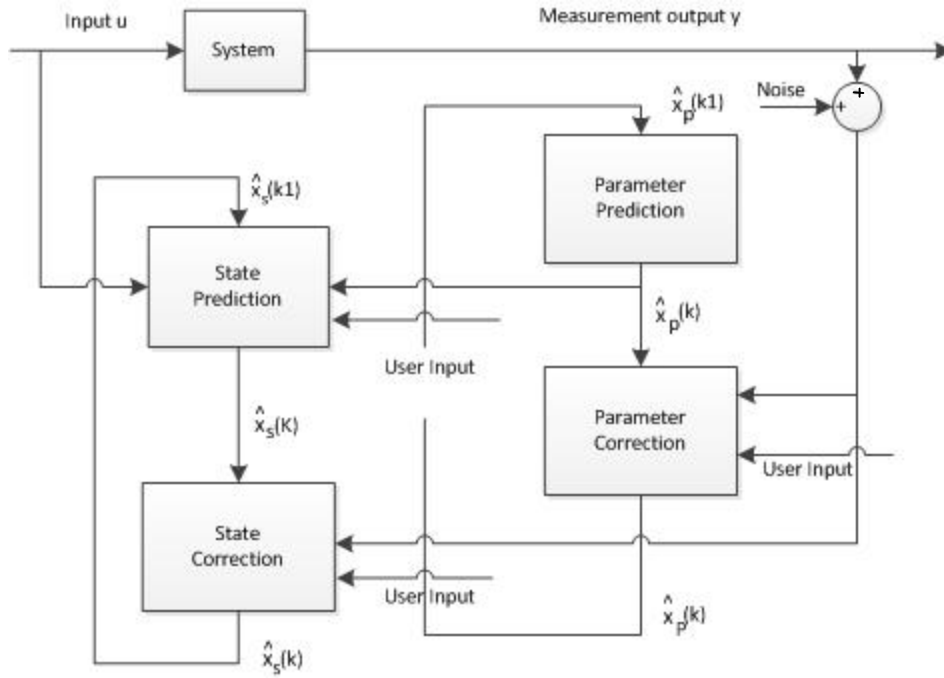
Figure 3.1. Scheme of the DEKF

The basic equations for the DEKF for such a non-linear system they are stated here as follows [31]:

Parameter prediction:

$$\hat{x}_p^-(k) = \hat{x}_p(k-1) \tag{3.44}$$

$$P_p^-(k) = P(k-1) + R_p \tag{3.45}$$

State prediction:

$$\hat{x}_s^-(k) = f(\hat{x}_s^-(k-1).u(k).\hat{x}_p^-(k)) \tag{3.46}$$

$$P_s^-(k) = F(k)P_s^-(k-1)F^T(k) + R_s \tag{3.47}$$

State correction:

$$K_s(t) = P_s^-(t)H_s^T(H_sP_s^-(t)H_s^T)^{-1} \tag{3.48}$$

$$\hat{x}_s(t) = \hat{x}_s^-(t) + K_s(t)(y(t) - H_s\hat{x}_s^-(t)) \tag{3.49}$$

$$P_s(t) = (I - K_s(t)H_s)P_s^-(t) \tag{3.50}$$

Parameter correction:

$$K_p(k+1) = P_p(k)H_p^T(H_pP_p(k)H_p^T)^{-1} \tag{3.51}$$

$$\hat{x}_p(k+1) = \hat{x}_p(k) + (K_p(k) + T_sS_kR_k^{-1})(y(k) - H_s\hat{x}_s(k)) \tag{3.52}$$

$$\begin{aligned}
P_p(k+1) = &\left(I - K_p(k)H_p\right)P_p(k) + T[Q_k - S_kR_k^{-1}S_k^T \\
&- S_kR_k^{-1}H_p(k)\left(\left(I - K_p(k)H_p\right)P_p(k)\right) \\
&+ \left(\left(I - K_p(k)H_p\right)P_p(k)\right)H_pR_k^{-1}S_k^T)]
\end{aligned} \tag{3.53}$$

where

$$Q(k) = (1-\alpha)Q(k) + \alpha\sigma^2w(k)w^T(k) \tag{3.54}$$

$$S(k) = (1-\alpha)S(k) + \alpha\sigma w(k)v(k) \tag{3.55}$$

$$R(k) = (1-\alpha)R(k) + \alpha v(k)v^T(k) \tag{3.56}$$

with

$$w(k) = \frac{1}{T_s}(\hat{x}_p(k) - \hat{x}_p(k-1)) \tag{3.57}$$

$$v(k) = y(k) - H_s \hat{x}_s(k) \tag{3.58}$$

Except for suitable nominal initial conditions for Q_k, R_k and S_k, two tuning parameters are now demanded, α and σ. For the instruction of a suitable memory of the error history into the covariance, α utilizes an exponentially weighted moving average to the propagation of the noise matrices. It can be better understood by means of the filtering time constant, τ it introduces, using

$$\alpha = 1 - e^{(T_s/\tau)} \tag{3.59}$$

Set in the range $0 \le \sigma \le 1$, the identification is stabilized through decreasing the error expectation in the change of parameters. The filter causes parameter adaptation, which induces (a desirable) non-zero $w(k)$. However, these changes are errors according to the zero model of Eq. 3.46, and if their total magnitude is interpreted as error, Q_k becomes relatively large compared with R_k, which results in an increase in the feedback gain K_k to provide greater correction to the u. Subsequent parameter corrections are then larger, and this induces instability. σ provides a means of balancing the filter such that the changes in Q_k are, correctly, not interpreted entirely as error [31].

Here, R_s and R_p are user-specified process noise covariance matrices for the state and parameter estimators, respectively, and, P_s and P_p are the covariance matrices of the estimation errors, respectively.

After defining the system dynamic equations $f(\cdot)$ and $h(\cdot)$, the Jacobian matrices F and H_s for the state and output equations are then given, respectively, by

$$F = \begin{bmatrix} \dfrac{\partial f_1}{\partial x_1} & \cdots & \dfrac{\partial f_1}{\partial x_m} \\ \vdots & \ddots & \vdots \\ \dfrac{\partial f_m}{\partial x_1} & \cdots & \dfrac{\partial f_m}{\partial x_m} \end{bmatrix} \tag{3.60}$$

$$H_s = \frac{\partial h}{\partial x_s} \tag{3.61}$$

The input vector u and the output vector y consist of the available measurable vehicle states:

$$y = H_s x_s \tag{3.62}$$

H_p equation is as follow:

$$H_p = H_s \frac{\partial f(\hat{x}_s, \hat{x}_p)}{\partial \hat{x}_p} \tag{3.63}$$

4. HANDLING RELATED STATE AND PARAMETER ESTIMATION

The Kalman filter and extended Kalman filter algorithm presented in this dissertation are used to estimate vehicle slip angle. The vehicle sideslip angle must be estimated as described below since it cannot be measured directly. The estimation of sideslip angle is therefore a critical part of the many active safety systems in vehicles. The vehicle sensor values are used in the estimation of sideslip angles as described below in this chapter. The axle slip angles may be calculated from the vehicle forward velocity, lateral velocity, yaw rate and front road wheel steer angle. Yaw rate and steering angle and forward velocity are measured directly, however sideslip angle must be estimated.

Kalman filter and extended Kalman filter algorithm approaches to estimate lateral velocity are presented in this chapter. Additionally the estimation of slip angle along with estimation of road friction coefficient and tire model parameters are presented.

4.1 Estimation of Linear Planar Vehicle states

The measured yaw rate sensor value may be considered output of the bicycle model described in chapter 2. The linear bicycle model may be reformulated as a stochastic model with zero-mean process random noise $w(t)$ and the measurement random noise $v(t)$.

$$\dot{x} = A_c x + Bu + w(t) \tag{4.1}$$

$$y = Cx + Du + v(t) \tag{4.2}$$

where

$$x = \begin{bmatrix} \beta \\ r \end{bmatrix} \tag{4.3}$$

$$y = r \tag{4.4}$$

$$A_c = \begin{bmatrix} \dfrac{-C_{\alpha f} - C_{\alpha r}}{m_v v_x} & -1 + \dfrac{C_{\alpha r} l_r - C_{\alpha f} l_f}{m_v v_x^2} \\ \dfrac{C_{\alpha r} l_r - C_{\alpha f} l_f}{I_z} & \dfrac{-C_{\alpha f} l_f{}^2 - C_{\alpha r} l_r{}^2}{I_z v_x} \end{bmatrix} \tag{4.5}$$

$$B = \begin{bmatrix} \dfrac{C_{\alpha f}}{m_v v_x} \\ \dfrac{C_{\alpha f} l_f}{I_z} \end{bmatrix} \tag{4.6}$$

$$C = \begin{bmatrix} 0 & 1 \end{bmatrix} \tag{4.7}$$

$$D = 0 \tag{4.8}$$

In this case the Kalman filter can be used to implement an optimal observer with respect to the noise characteristics of w(t) and v(t). To implement the Kalman filter, the auto-covariance matrices of w(t) and v(t) must be specified:

$$Q = E\{w.w^T\} \tag{4.9}$$

$$R = E\{v.v^T\} \tag{4.10}$$

In theory the process noise and measurement noise would be measured and the auto-covariances computed directly. In practice this is very difficult to do, especially for the process noise $w(t)$ as this often cannot be measured directly. As a result the Q and R matrices may be considered to be tuning parameters for the Kalman filter. Q and R matrices were specified as diagonal matrices with equal values along the diagonal of each.

$$Q = Q\mathrm{I} \tag{4.11}$$

$$R = R\mathrm{I} \tag{4.12}$$

This simplistic approach was used to "tune" the Kalman filter by the relative weighting of the scalar values Q and R.

In these simulations, vehicle is designed at small steering angle (sinusoid wave and step function). Other parameters are shown in Table A.2 in Appendix. Weighting of scalar values of Q and R are 0.001 and 0.005, respectively.
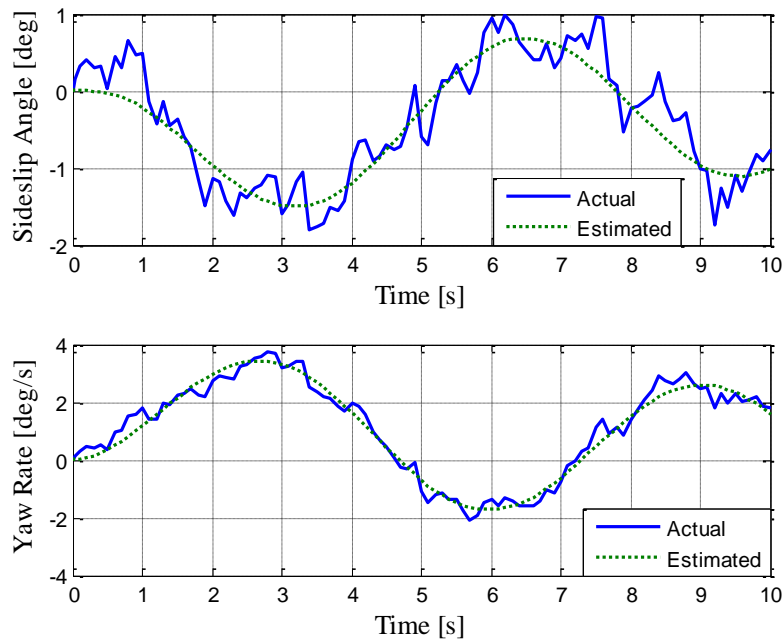
Figure 4.1. Estimation of sideslip angle and yaw rate, steering input sinusoid wave, amplitude 10 deg, velocity 30 m/s
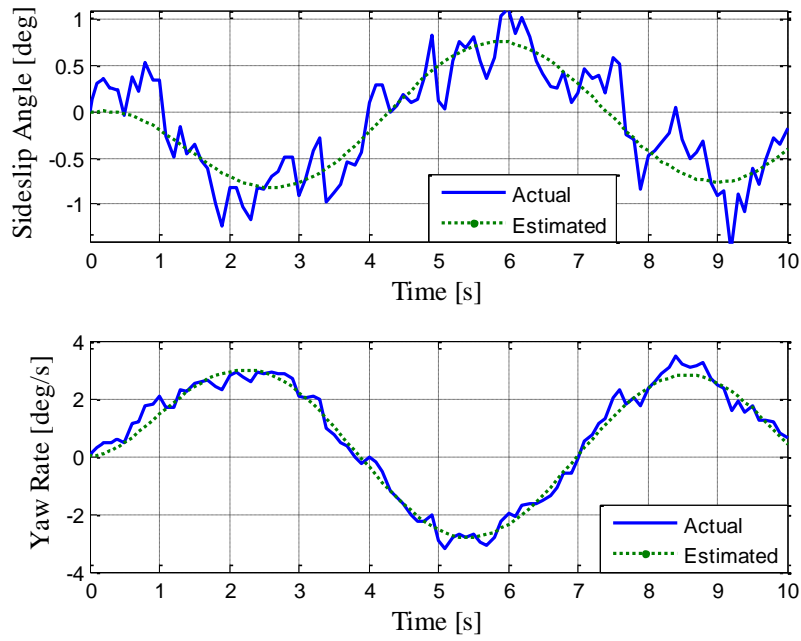
Figure 4.2. Estimation of sideslip angle and yaw rate, steering input sinusoid wave, amplitude 15 deg, velocity 20 m/s
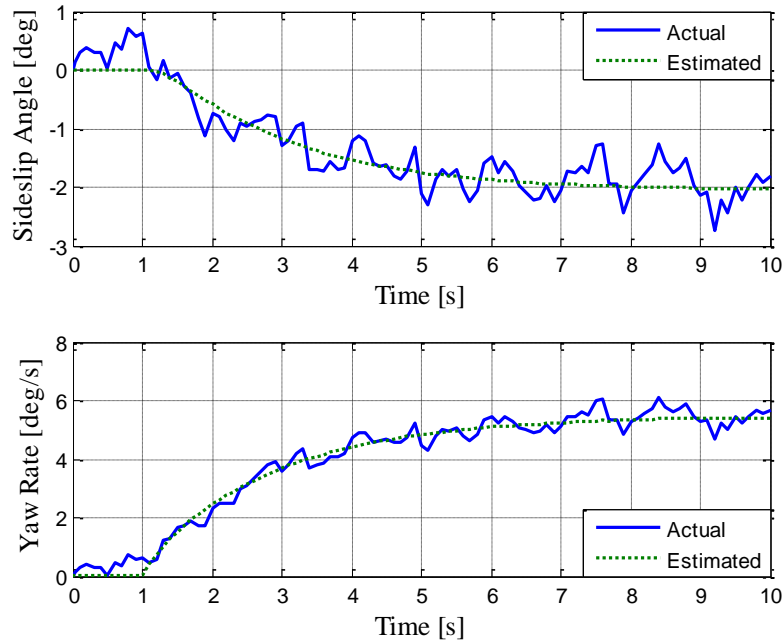

Figure 4.3. Estimation of sideslip angle and yaw rate, steering input step function, amplitude 12 deg, velocity 25 m/s

As a result the estimated sideslip angle in bicycle model is close to the actual one where the vehicle sideslip angle is not large value. Also, simulation results show

that Kalman filter method could reduce noise in measurement and estimation signals truly.

4.2. Estimation of Non-linear vehicle states

It has been shown in the chapter 3 that extended Kalman filter can be used to estimate the states of a system of interest from the noisy observation signals. It should be noted that if the noise free signals are available, the algorithms can also be used to obtain the system's parameters. The latter is sometimes referred to as a parameter estimation or system identification.

The state matrix presented here is based on four-wheel non-linear vehicle model. The state matrix consists of yaw rate r, lateral velocity v_y and lateral acceleration a_y based on measurements of lateral acceleration a_y, steer angle δ, vehicle speed v_x, and yaw rate r.

In this dissertation, the following simplifying assumptions was taken into account: the concentration on lateral force generation of tires; ignorance of dependence on longitudinal slip and setting up of the Magic Formula tire model as an exact model of tire force generation to which will be tried to fit a sufficient Rational tire model.

If the extended Kalman filtering method is used for the data estimation then it is necessary to formulate the system model in discrete state-space form. The differential equation discrete time of lateral acceleration is as follow:

$$a_y(k+1) = \frac{1}{m_v}(F_{y1}(k)\cos(\delta) + F_{y2}(k)\cos(\delta) + F_{y3}(k) + F_{y4}(k)) \qquad (4.13)$$

Discrete time Yaw rate can be obtained from:

$$r(k+1) = r(k) + T_s[\frac{1}{I_z}(l_f(F_{y1}(k)\cos(\delta) + F_{y2}(k)\cos(\delta)) - l_r(F_{y3}(k) +$$

$$F_{y4}(k)) + \frac{t}{2}(F_{y1}(k)\cos(\delta) + F_{y2}(k)\cos(\delta))] \qquad (4.14)$$

Discrete time lateral velocity can be obtained from:

$$v_y(k+1) = v_y(k) + T_s(a_y(k) - r(k)v_x(k)) \qquad (4.15)$$

In the above, t, k and T_s denotes track width, number of iteration and represents sample time which is 0.005, respectively

The lateral velocity, the steer angle of the front wheels and the yaw rate are then utilized as a basis for the calculation of the tire slip angles α_i as well as the vehicle body slip angle β:

$$\alpha_{1,2}(k) = \delta - \left(\frac{v_y(k)}{v_x(k)}\right) - \left(\frac{l_f r(k)}{v_x(k)}\right) \tag{4.16}$$

$$\alpha_{3,4}(k) = -\left(\frac{v_y(k)}{v_x(k)}\right) + \left(\frac{l_r r(k)}{v_x(k)}\right) \tag{4.17}$$

$$\beta(k) = \arctan\left(\frac{v_y(k)}{v_x(k)}\right) \tag{4.18}$$

the vertical forces can be calculated as follows:

$$F_{z1,2}(k) = \frac{l_r/2}{(l_f + l_r)} m_v g \pm m_v \frac{a_y(k) h_{CG} l_r}{t(l_f + l_r)} \tag{4.19}$$

$$F_{z3,4}(k) = \frac{l_f/2}{(l_f + l_r)} m_v g \pm m_v \frac{a_y(k) h_{CG} l_f}{t(l_f + l_r)} \tag{4.20}$$

where l_f and l_r are the distances to the front axle and the rear axle; h_{CG} is the height of center of mass [19].

In this chapter DEKF is used to estimate unmeasurable states and unknown parameters. This observer is designed and tested against data from a source model which employs Magic Formula tire model. For this work, we use rational tire model to generate lateral tire forces. Rational tire model depends on two parameters and road friction coefficient which vary with the different road surfaces.

To estimate states accurately such as sideslip angle and lateral tire forces, which have strong correlation with tire model, it is crucial to estimate these parameters and road friction coefficient precisely in any road surfaces. Hence dual extended Kalman filter (DEKF) which two EKF are used in parallel to estimate states and parameters which is shown in Figure 4.4. The study also presents the effect of number of measurements in this application and it concludes with a discussion in this chapter.

In this section three different simulations have been modified, one of which consist of using DEKF to estimate states alongside rational tire model parameters and friction coefficient based on measurement of yaw rate and lateral acceleration. The other one is using EKF for estimation of states without parameter estimation based on two which are yaw rate and lateral acceleration. And the last one is using EKF to estimate states without parameter estimation based on only measurement of yaw rate.
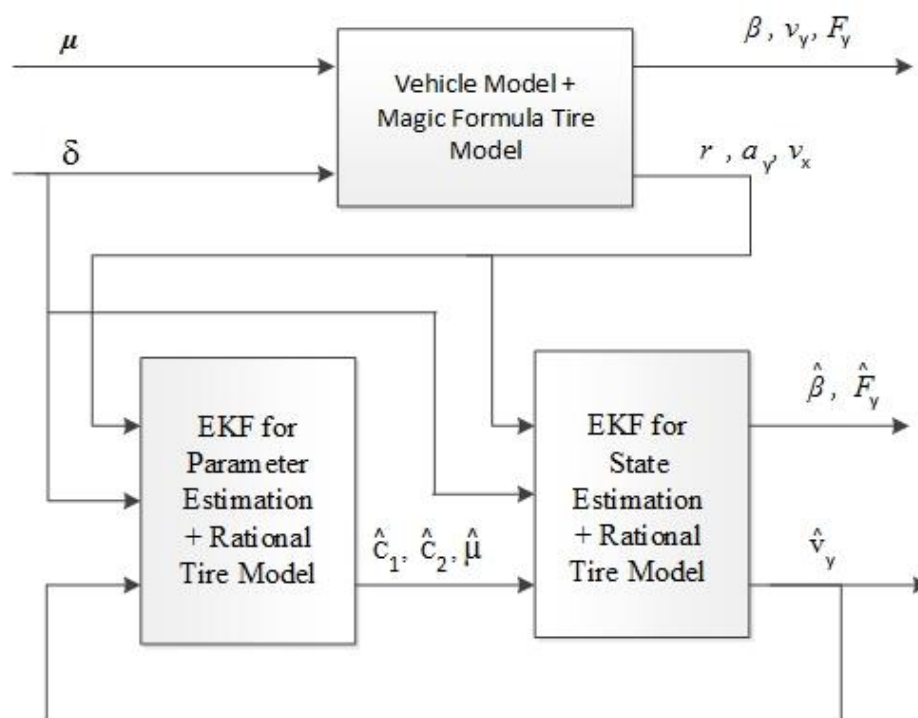

Figure 4.4. Simple representation of the simulation model incorporating non-linear vehicle models with Magic Formula/rational tire models and DEKF

The input vector u and the output vector y consist of the available measurable states:

$$u = \begin{bmatrix} \delta \\ v_x \end{bmatrix} \tag{4.21}$$

$$y = \begin{bmatrix} r \\ a_y \end{bmatrix} = H_s x_s \tag{4.22}$$

The state and parameter vectors form the internal states required by the dynamics safety control systems and the unknown tire model parameters, respectively:

$$x_s = \begin{bmatrix} r \\ v_y \\ a_y \end{bmatrix} \tag{4.23}$$

$$x_p = \begin{bmatrix} c_1 \\ c_2 \\ \mu \end{bmatrix} \tag{4.24}$$

where c_1 and c_2 are the Rational tire model constant parameters and μ is road friction coefficient.

Note that the matrix H_p is required, which can be simplified as follows:

$$H_p = H_s \frac{\partial f(\hat{x}_s, \hat{x}_p)}{\partial \hat{x}_p} = \begin{bmatrix} \dfrac{\partial r}{\partial c_1} & \dfrac{\partial r}{\partial c_2} & \dfrac{\partial r}{\partial \mu} \\ \dfrac{\partial a_y}{\partial c_1} & \dfrac{\partial a_y}{\partial c_2} & \dfrac{\partial a_y}{\partial \mu} \end{bmatrix} \tag{4.25}$$

4.2.1 Simulations

In these simulations, the vehicle was assumed that it experienced a maneuver subject to Fishhook and sinusoid wave steering input, which is shown in Figure 4.5 and 4.6, respectively, on the road with various friction coefficients and other parameters in vehicle is shown in Table A.3 in Appendix.
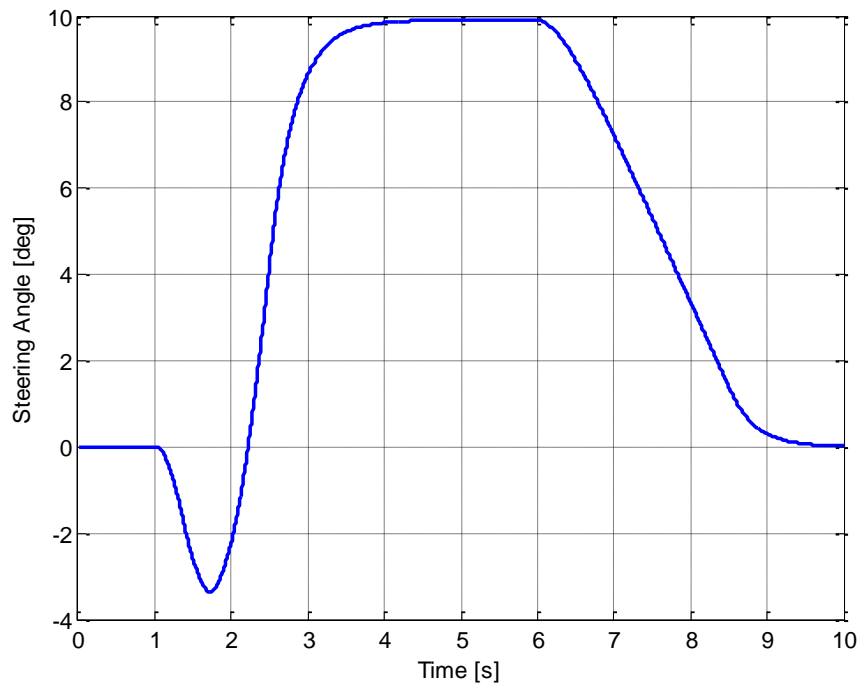
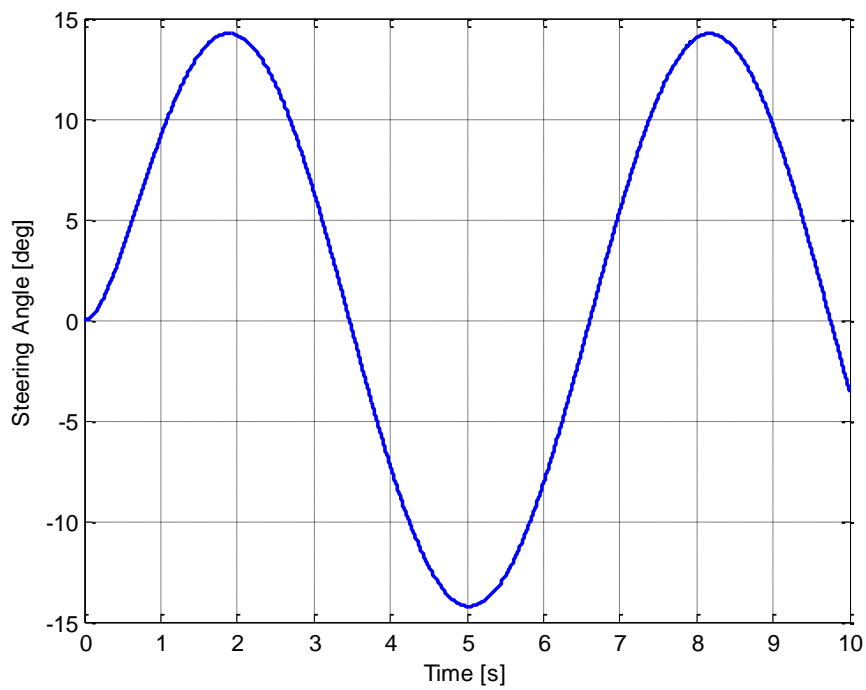Figure 4.5. Fish-hook steering angle input used in simulations

Figure 4.6. Sinusoid wave steering angle input used in simulations

In the first simulation, a DEKF algorithm is used to estimate states alongside rational tire model parameters and friction coefficient based on measurement of yaw rate and lateral acceleration.

In the second simulation, an EKF is used for the estimation of states without parameter estimation based on yaw rate and lateral acceleration measurements.

In the third, simulation an EKF algorithm is used to estimate states without any parameter estimation based on measurement of yaw rate only.

Estimation of states of three different conditions, which is explained above, for various road surfaces and different steering angle inputs are shown in figures below.

Note that all figures of rational tire model c_1 , c_2 parameters and road friction coefficient are related to DEKF algorithm.
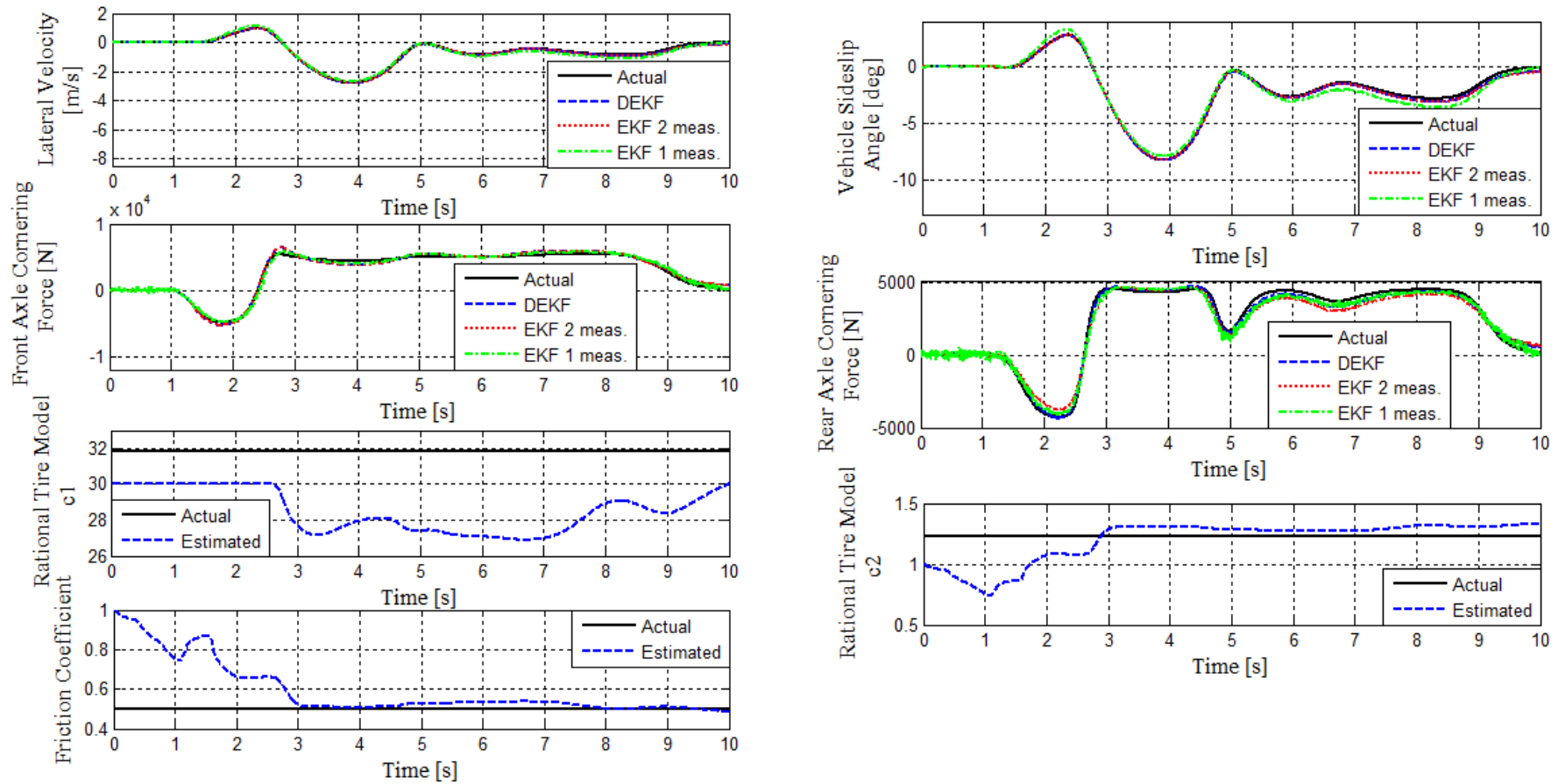
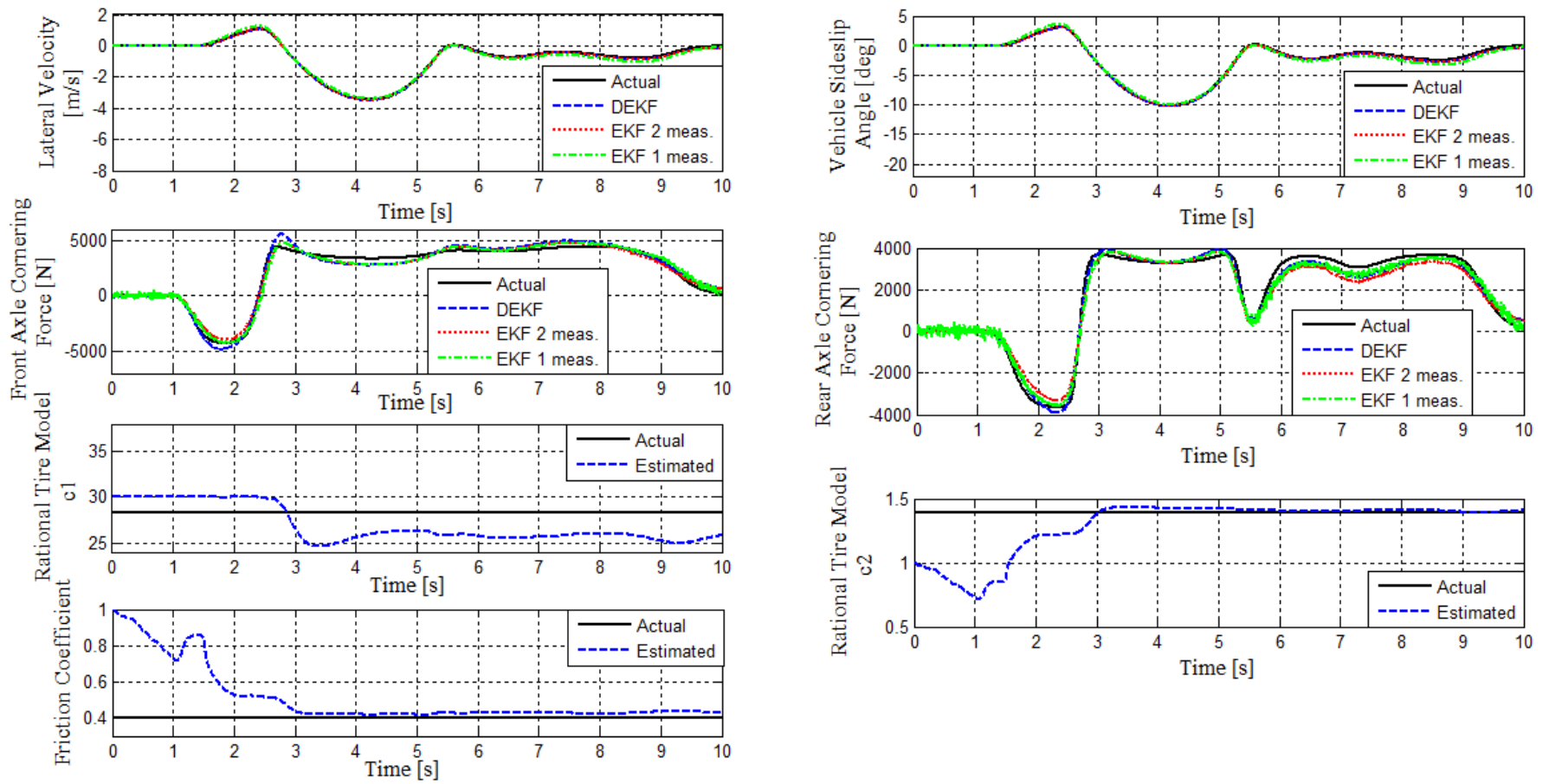Figure 4.7. Simulations and estimations corresponding to road friction coefficient μ=0.5 at fishhook steering angle

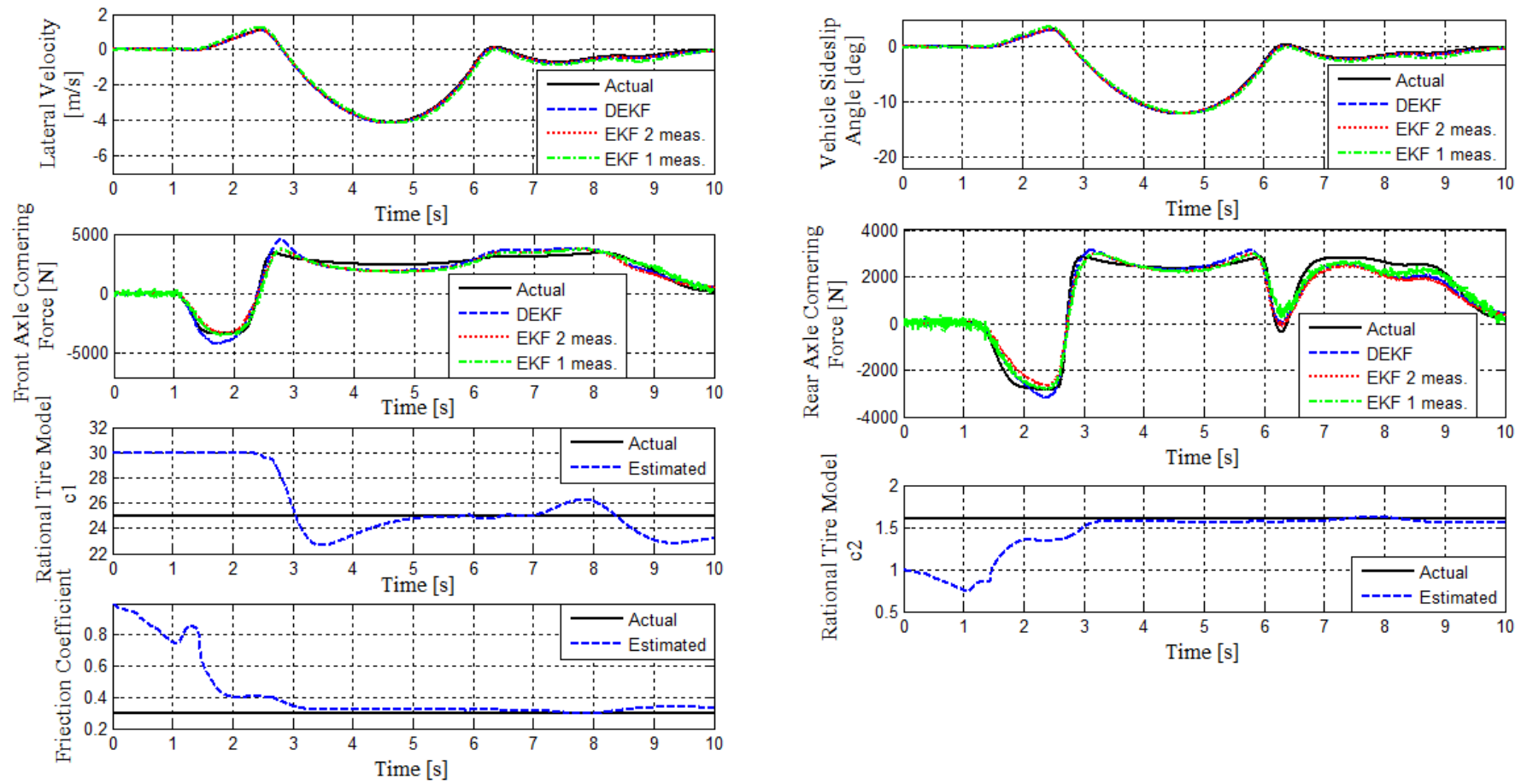Figure 4.8. Simulations and estimations corresponding to road friction coefficient μ=0.4 at fishhook steering angle

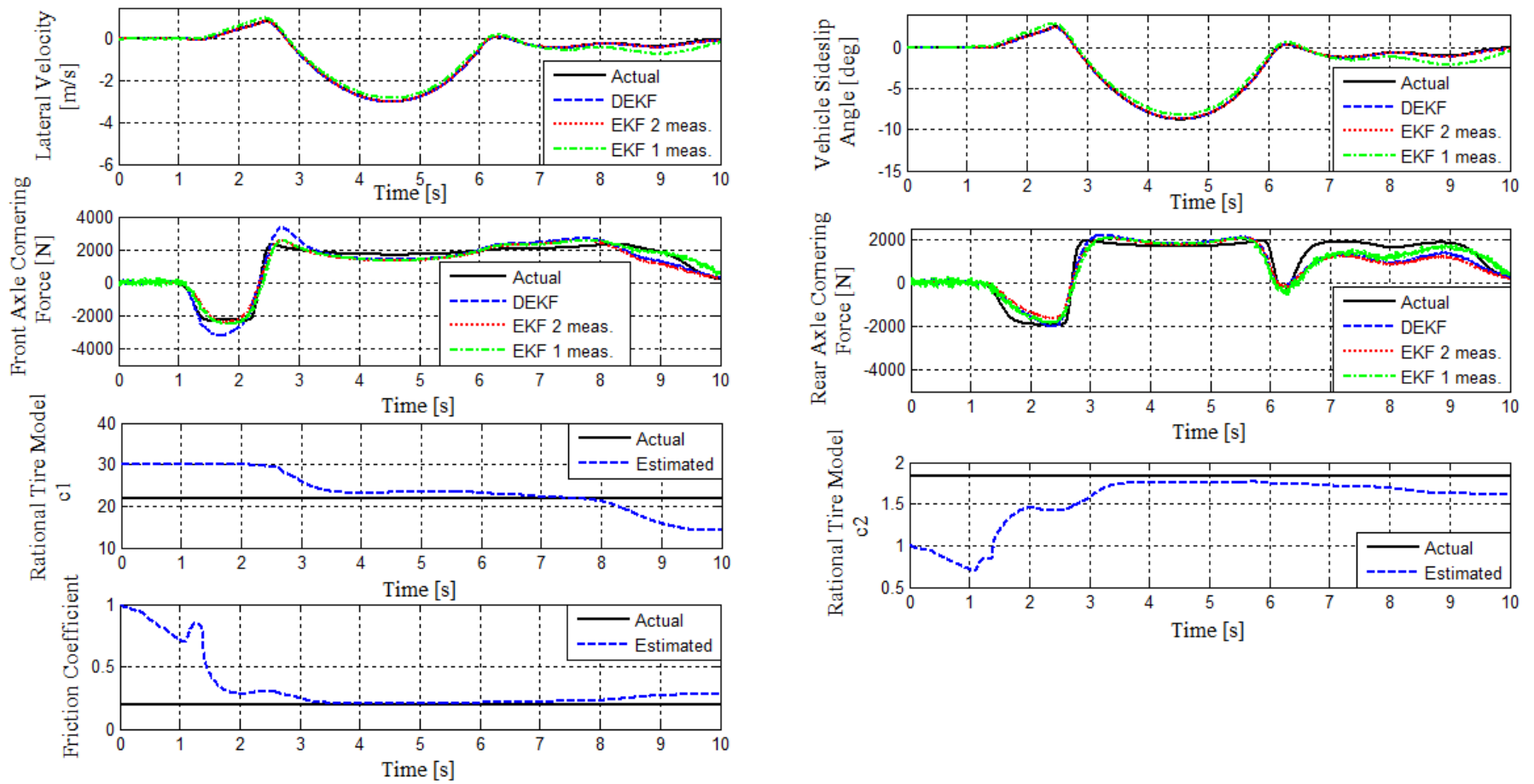Figure 4.9. Simulations and estimations corresponding to road friction coefficient μ=0.3 at fishhook steering angle

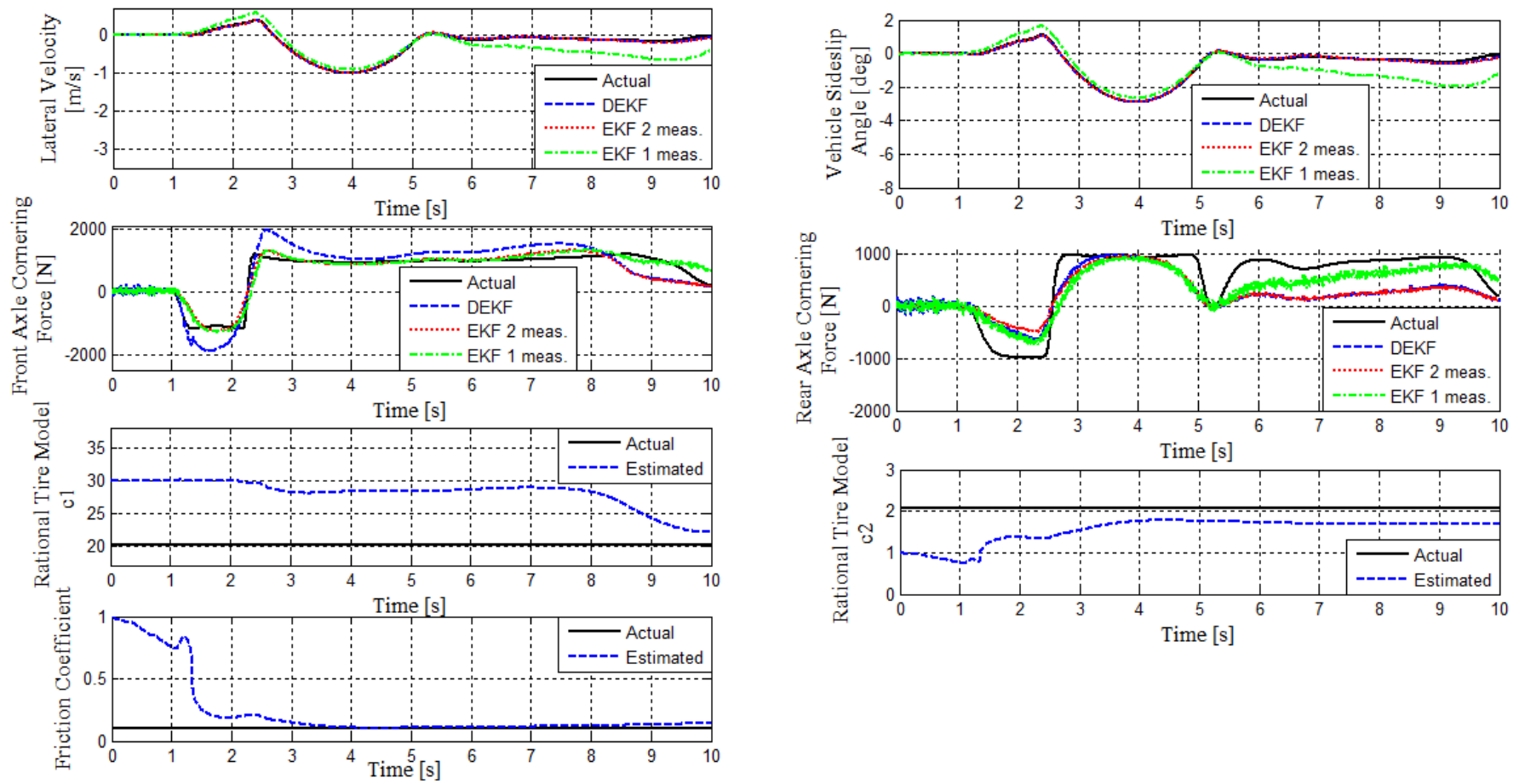Figure 4.10. Simulations and estimations corresponding to road friction coefficient μ=0.2 at fishhook steering angle

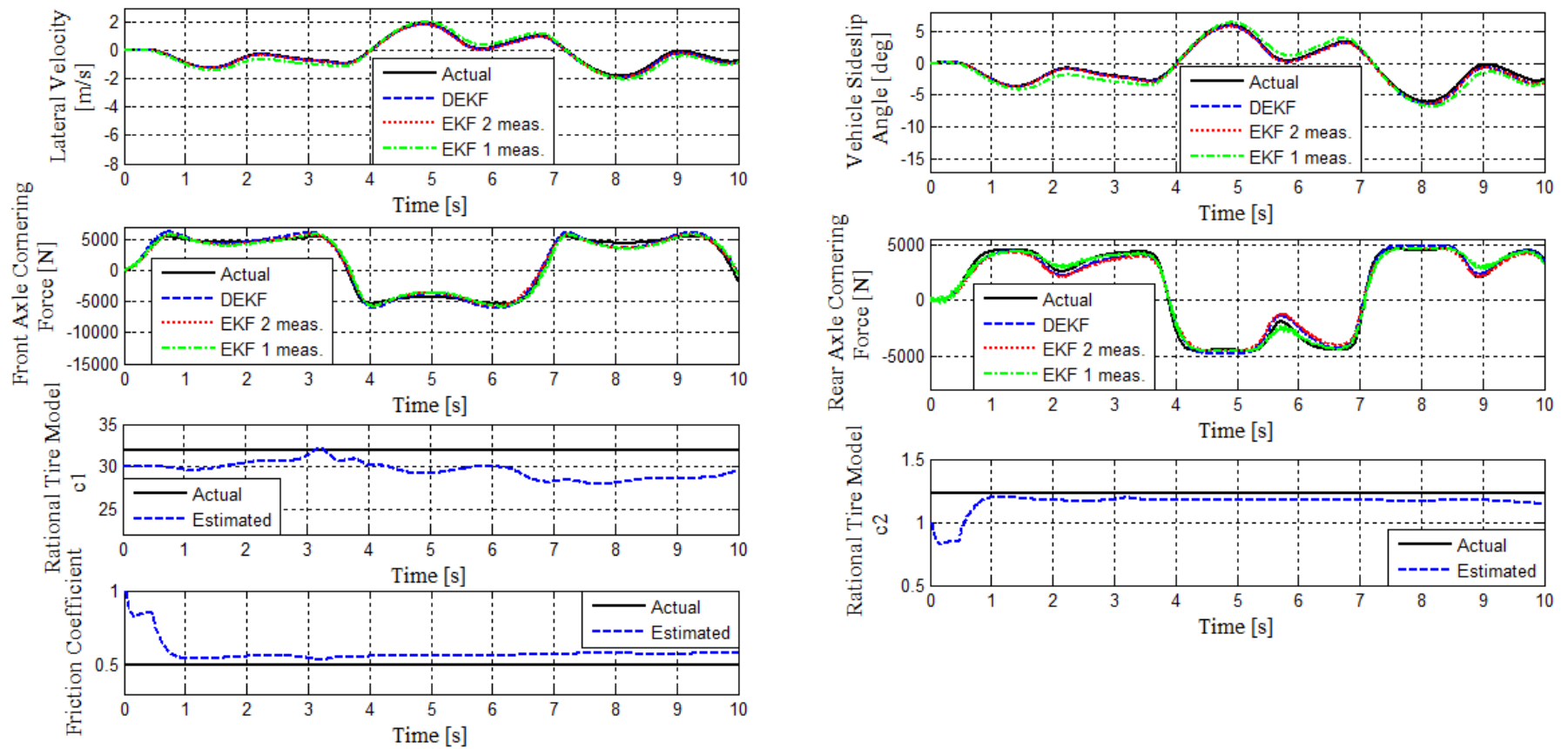Figure 4.11. Simulations and estimations corresponding to road friction coefficient µ=0.1 at fishhook steering angle

Figure 4.12. Simulations and estimations corresponding to road friction coefficient μ=0.5 at sinusoid wave steering angle

Figure 4.13. Simulations and estimations corresponding to road friction coefficient μ=0.4 at sinusoid wave steering angle

Figure 4.14. Simulations and estimations corresponding to road friction coefficient μ=0.3 at sinusoid wave steering angle
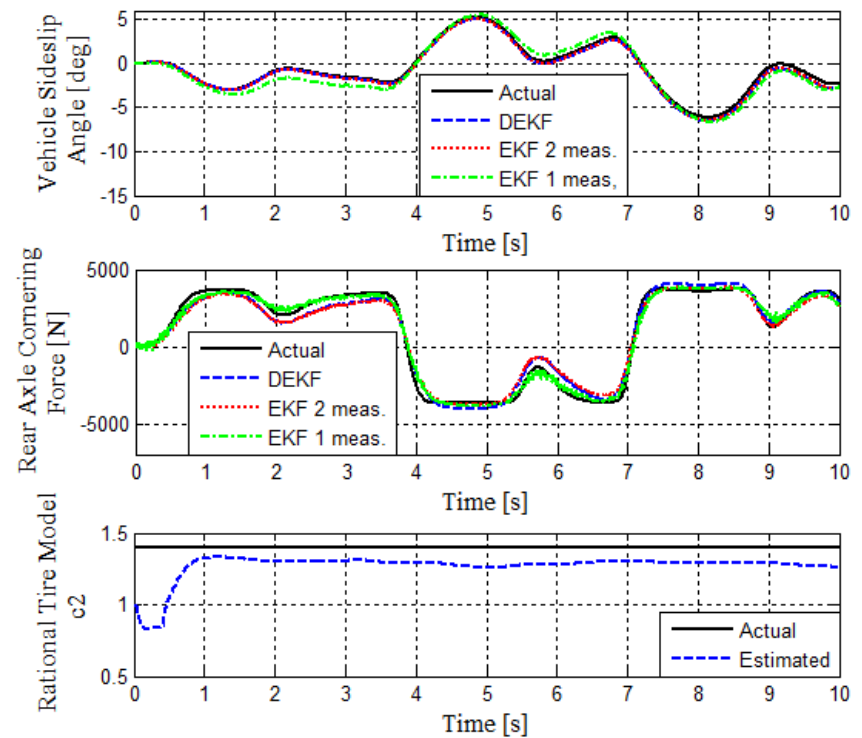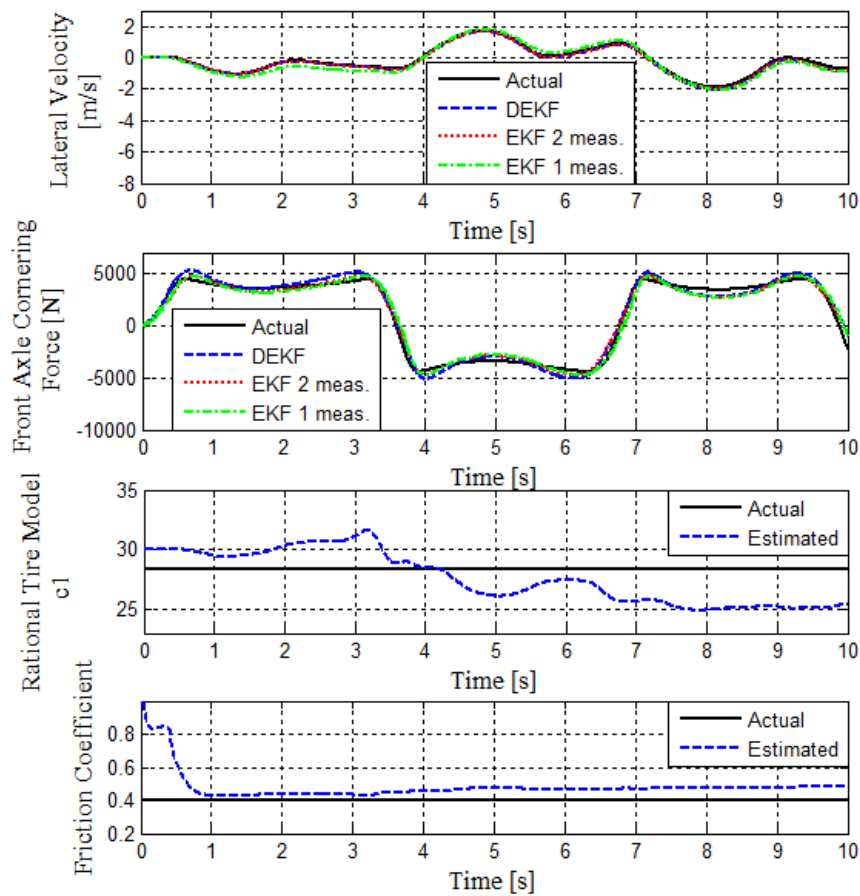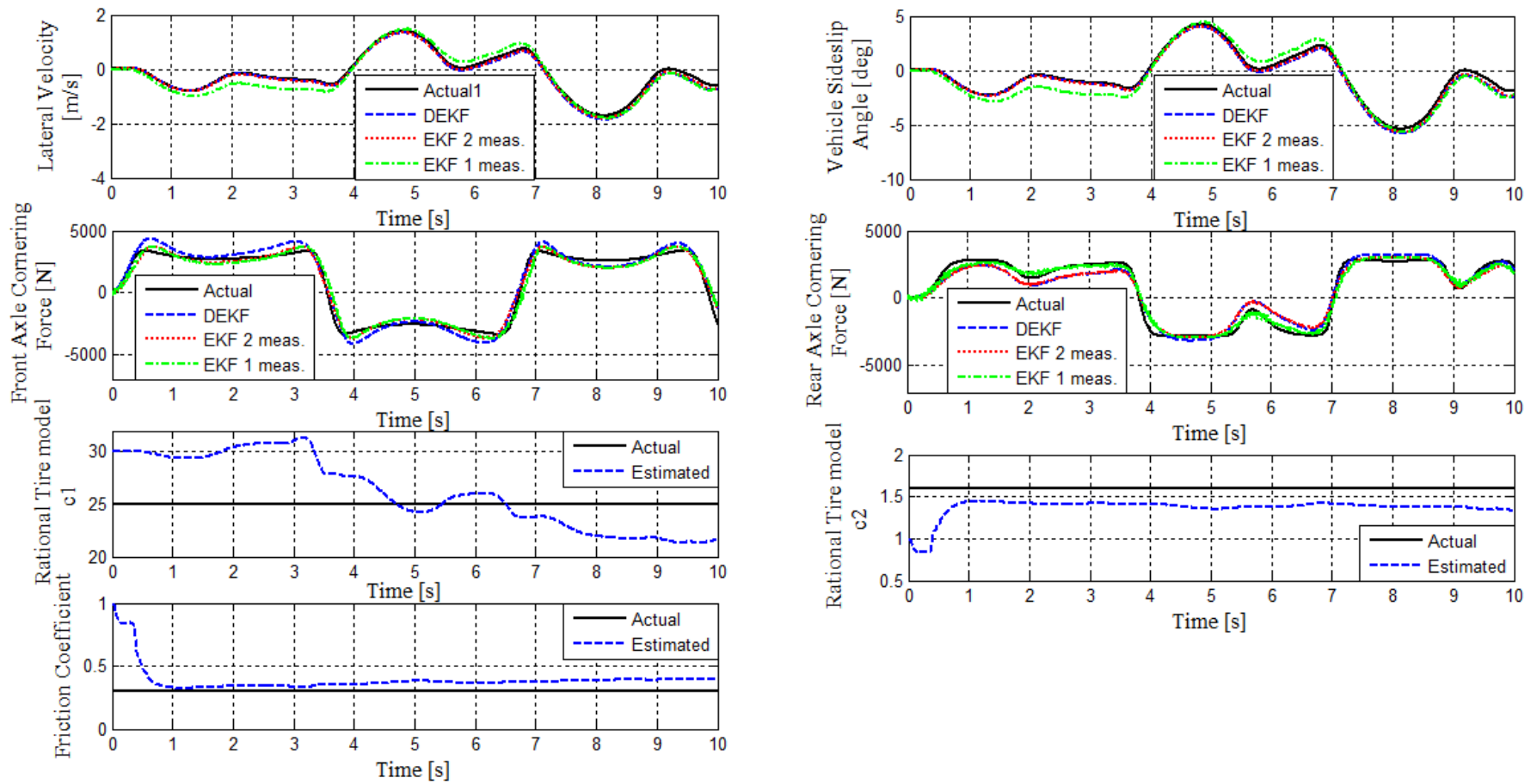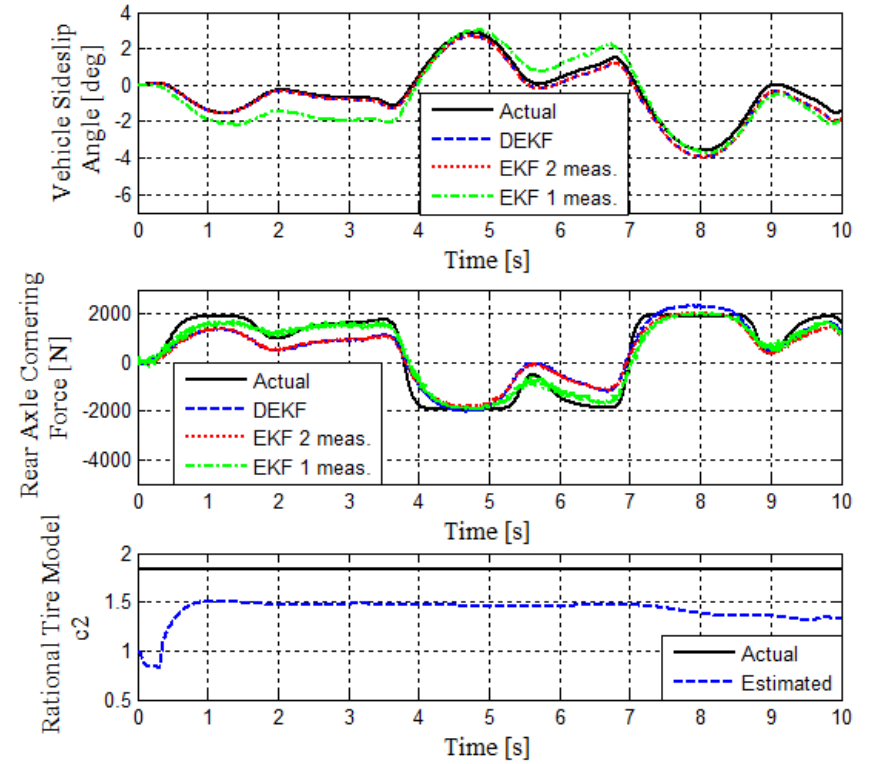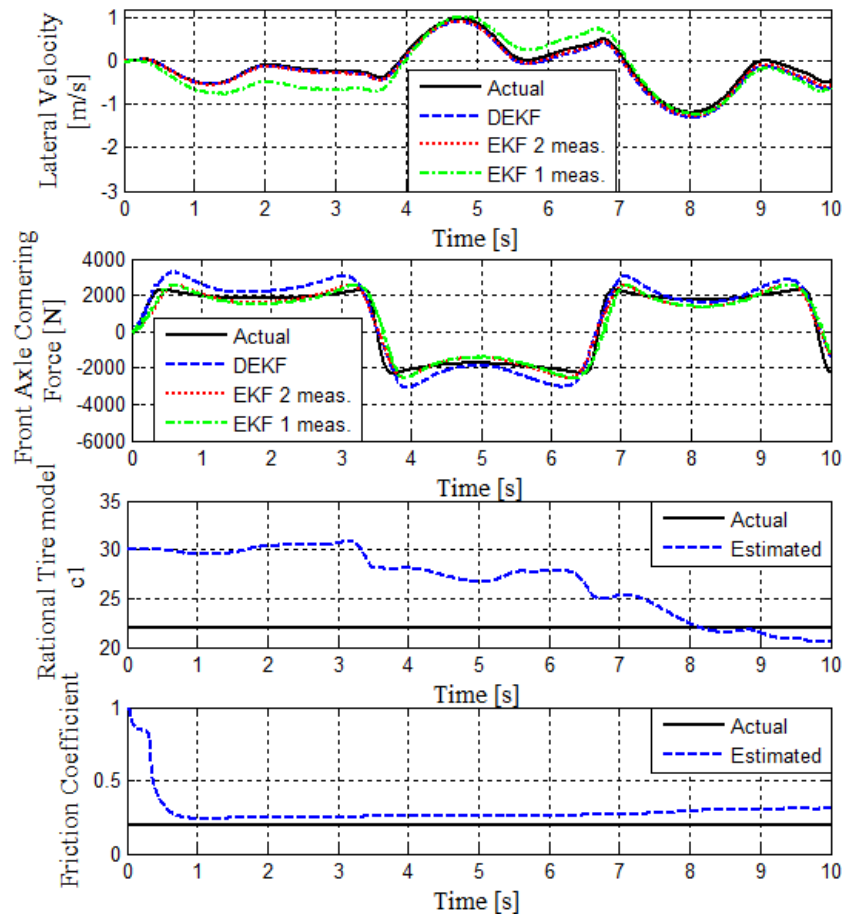
Figure 4.15. Simulations and estimations corresponding to road friction coefficient μ=0.2 at sinusoid wave steering angle
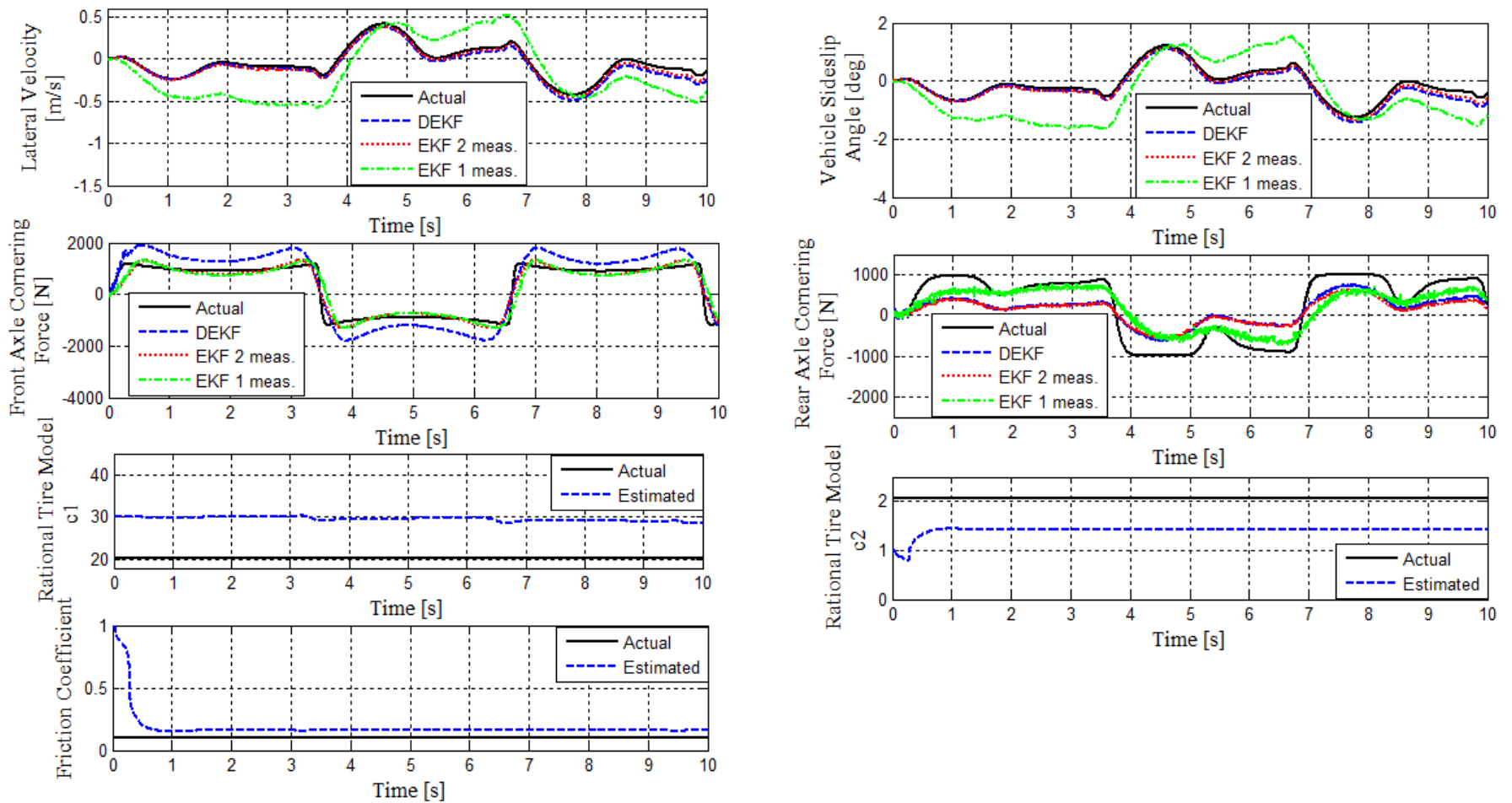
Figure 4.16. Simulations and estimations corresponding to road friction coefficient μ=0.1 at sinusoid wave steering angle

It can be seen from the simulation results that all the estimators give the reasonable results for vehicle sideslip angle. However, DEKF algorithms seem to give better results.

The estimation of the front/rear axle cornering forces of three simulations has the sufficient accuracy to acquire sideslip angle and lateral velocity with high precision.

4.3 Conclusions

This chapter has provided application of Kalman filter and extended Kalman filter for estimation in linear and non-linear planer vehicle model. Results of estimation are shown in this chapter.

Moreover, this chapter introduced effective algorithms to estimates friction coefficient and tire model parameters which cause tire model is adaptive for any road surfaces.

The Kalman filtering method for sideslip angle of the vehicle is proposed in this chapter which is based on the non-linear vehicle model and the modified Rational tire model. It has realized the observing the vehicle sideslip angle and friction coefficient on-line via the signal from source model. The simulation results indicate that this algorithm can be calculated in real-time on various road surfaces.

Therefore, the extended kalman filter observer in this chapter is proposing a low-cost and more practical idea for estimating the vehicle sideslip angle, friction coefficient and tire model parameters on-line estimation.

5. WHEEL SLIP REGULATION RELATED STATE AND PARAMETER ESTIMATION

5.1 Introduction

Wheel slip, which is defined in Eq. 2.2, is a dimensionless measure of the difference between the vehicle speed v and the circumferential speed ωW_r of the wheel relative to its center. We take as convention that $v > 0$ and $0 \leq \omega W_r \leq v$ for braking, where $v = \omega W_r$ only at the onset of braking [21]. In the steady-state, there are two possible cases: (1) Finite rotation of the wheel ($\omega W_r \neq 0$) while the vehicle decelerates with $\lambda \in (0,1)$ and (2) deceleration under lockup conditions ($\omega W_r = 0$) with $\lambda = 1$.

The wheel slip must be very accurately calculated. Due to the extremely high gradient of the cohesion coefficient characteristics, errors in the per-thousands range can result in force reactions of considerable dimensions.

The primary objective of the slip controller is to bring a car traveling with an initial speed v_0 down to stop in a shortest possible distance or time while using admissible control ($0 \leq T_b \leq T_{b_{max}}$). In doing so the slip value should rise to its optimum value λ_0 as fast as possible and track this value through the deceleration process with minimal deviation from the set reference value λ_0 until the car stops. The braking system should also use admissible braking torques, i.e. have limited control input through the braking process including initial transient response, steady state control and the final stage of the braking process as the car comes to rest [32].

The second aim of wheel slip regulation is to adapt tire on various road surfaces. Therefore, tire model updating for road surfaces plays a crucial role to generate true value of tire forces.

5.2. Close Loop Control Systems

Control system engineers are concerned with controlling a part of an environment known as a plant or system in order to produce desired products for society. A prior knowledge of the plant to be controlled is often critical in designing effective control systems. The application of different engineering principles like that of electrical,

mechanical, and/or chemical in order to achieve the desired output make control engineering a multi-faceted engineering domain [33].

In closed-loop control systems the difference between the actual output and the desired output is fed back to the controller to meet desired system output. Often this difference, known as the error signal is amplified and fed into the controller. Figure 2 shows the general structure of a closed-loop feedback control system. A few examples of feedback control systems are elevators, thermostats, and the cruise control in automobiles [33].
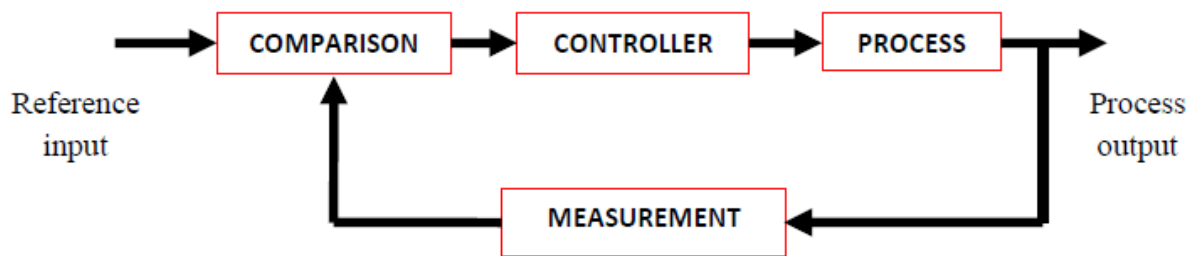
Figure 5.1. Closed loop control system [33].

5.2.1 PI Controller

In control engineering, a PI Controller (proportional-integral controller) is a feedback controller which drives the plant to be controlled by a weighted sum of the error (difference between the output and desired set-point) and the integral of that value. It is a special case of the PID controller in which the derivative (D) part of the error is not used [33].

The PI controller is mathematically denoted as:

$$G_c = K_p + \frac{K_i}{s} = k_p(1 + \frac{1}{sT_i})$$ (5.1)

Figure 5.2. PI controller scheme [34]

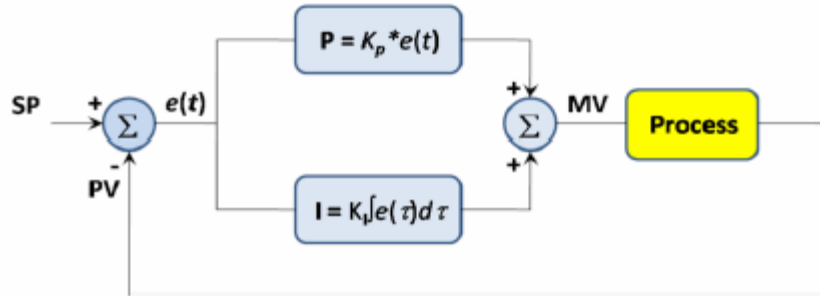Integral control action added to the proportional controller converts the original system into high order. Hence the control system may become unstable for a large value of k_p since roots of the characteristic equation may have positive real part. In this control, proportional control action tends to stabilize the system, while the integral control action tends to eliminate or reduce steady-state error in response to various inputs. As the value of Ti is increased,

☐ Overshoot tends to be smaller

☐ Speed of the response tends to be slower.

5.3. Wheel Slip Regulation Using DEKF

This chapter describes a PI controller and Extended Kalman filtering technique which employs an additional angular velocity sensor to complement the wheel-based speed sensor, and produce an accurate estimation of the true speed of a vehicle. We use the Extended Kalman filters to deal with the noise and uncertainties in the speed, and to tune the covariance and reset the initialization of the filter according to slip conditions detected and measurement-estimation condition. Magic Formula is employed in quarter car braking model as a source model to verify the proposed strategy. Also, estimation of the tire model parameters is significant since tire must be adaptive for any tire road surfaces. Here, Burckhardt tire model is chosen. Therefore, using DEKF for estimation states alongside parameters as shown in Figure 5.2.

A model for single wheel braking is described in chapter 2. There may be other forces that act on a braked vehicle that influence its deceleration, including driveline drag,

grade, rolling resistance, and aerodynamic drag [3], but these are not considered here
[3].

Discretizing the equations of quarter car braking model for using DEKF can be
obtained below.

Discrete time wheel angular velocity and vehicle velocity and wheel slip can be
obtained from:

$$\omega(\mathrm{k}+1) = \omega(\mathrm{k}) + \frac{\mathrm{T_s}}{\mathrm{J}}\left(\mathrm{W_r}\mathrm{F_x}(\mathrm{k}) - \mathrm{sign}\big(\omega(\mathrm{k})\big)\mathrm{T_b}\right) \tag{5.2}$$

$$V_\mathrm{x}(\mathrm{k}+1) = V_\mathrm{x}(\mathrm{k}) - \frac{\mathrm{T_s}}{\mathrm{m}}\mathrm{F_x}(\mathrm{k}) \tag{5.3}$$

$$\lambda(k) = \frac{V_\mathrm{x}(k) - W_r\omega(k)}{V_\mathrm{x}(k)} \tag{5.4}$$

The algorithm of DEKF is shown in Figure 5.3. $\mathrm{T_s}$ for this simulation is considered as
0.005. Parameters of quarter car model are shown in Table A.4 in Appendix.

The input vector u and the output vector y consist of the available measurable states:

$$u = [T_b] \tag{5.5}$$

$$y = [\omega] = H_s x_s \tag{5.6}$$

The state and parameter vectors form the internal states required by the quarter car
braking system and the unknown tire model parameters, respectively:

$$x_s = \begin{bmatrix} \omega \\ v \end{bmatrix} \tag{5.7}$$

$$x_p = \begin{bmatrix} c_1 \\ c_2 \end{bmatrix} \tag{5.8}$$

where c_1 and c_2 are Burckhardt tire model parameter which is described in section 2.3.2. In this chapter we ssumed that the Burckhardt tire model c_3 parameter is fixed $(c_3 = 0.5)$.

Note that the matrix H_p is required, which can be simplified as follows:

$$H_p = H_s \frac{\partial f(\hat{x}_s, \hat{x}_p)}{\partial \hat{x}_p} = \begin{bmatrix} \dfrac{\partial \omega}{\partial c_1} & \dfrac{\partial \omega}{\partial c_2} \end{bmatrix} \tag{5.9}$$
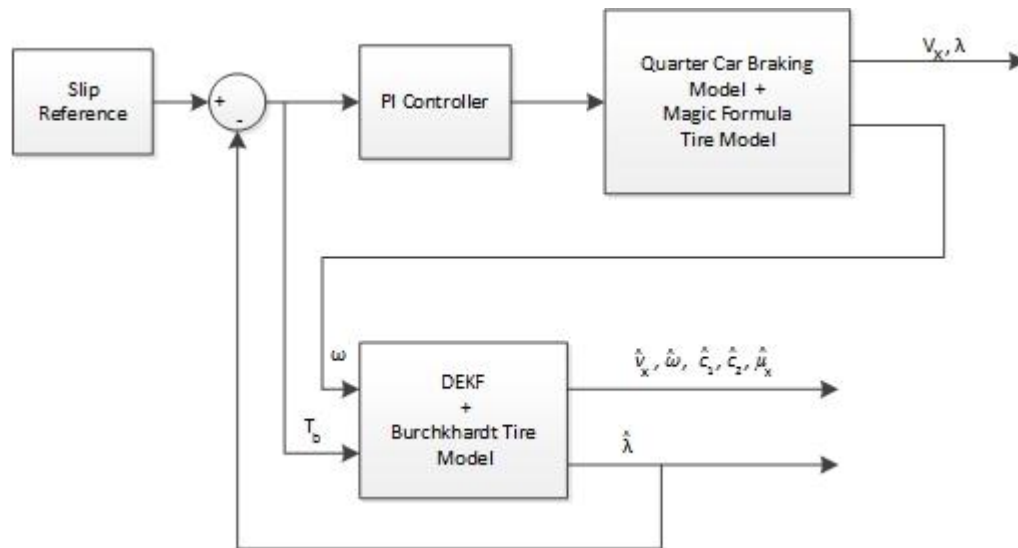

Figure 5.3. Wheel slip Regulation with Burckhardt tire model

In these simulations, five situations were studied for wheel slip regulation.

As seen in Figure 5.4, vehicle travels from wet road to dry road. The estimation of longitudinal velocity and dynamic friction coefficient are quite well. Longitudinal slip is tracking reference signal and parameters identification for c_1 and c_2 are acceptable.

In Figure 5.5, snow-dry transitioning, the accuracy of estimation of longitudinal velocity, dynamic friction coefficient and parameter c_1 are high but the estimation of parameter c_2 is poor. The initial value for parameter c_2 has not changed during traveling from snow road to dry road.

As detailed in Figure 5.6 and Figure 5.7, estimation of longitudinal velocity and dynamic friction coefficient are precise.

As depicted in Figure 5.8, all of the states are estimated well but parameter identifications for c_1 and c_2 are not precise. This problem happens because environment changes abruptly and linearization of jacobian matrics can not be done.

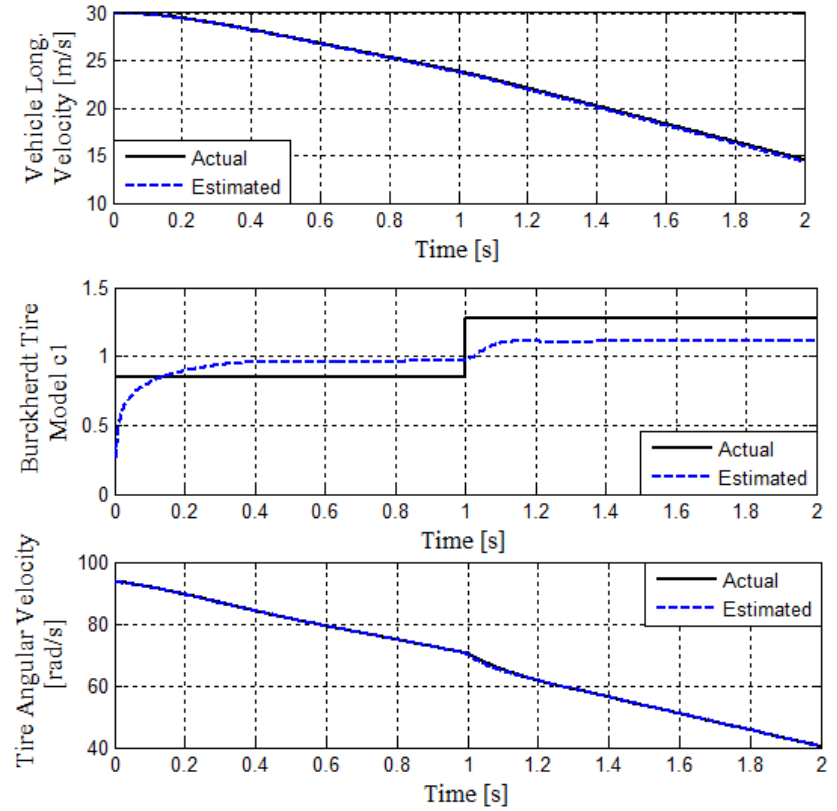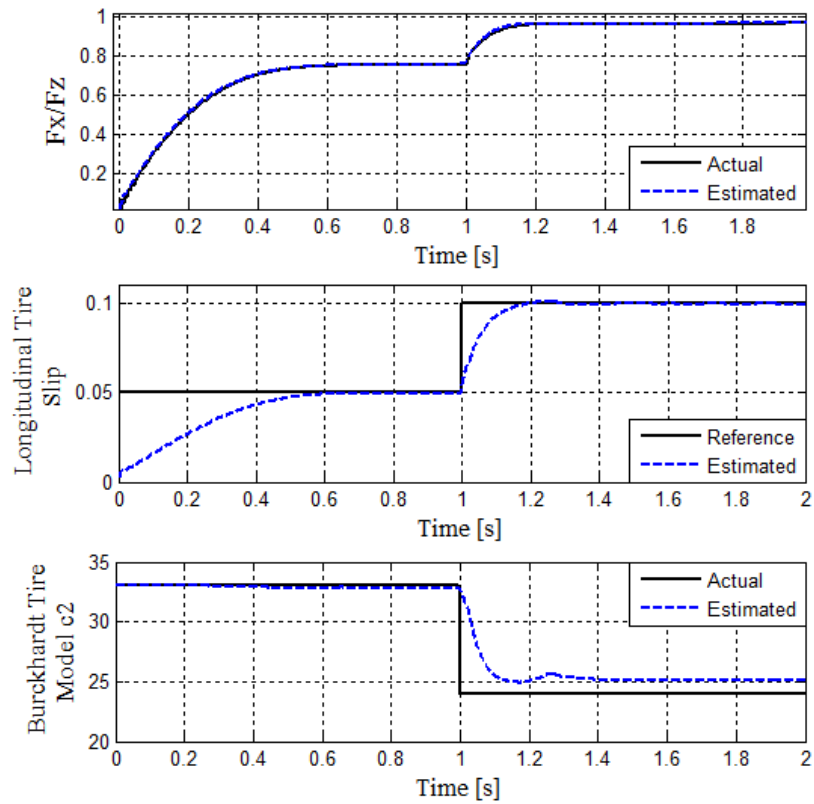Simulation results show in figures below:

Figure 5.4. Wheel slip regulation simulation results during wet-dry road transitioning
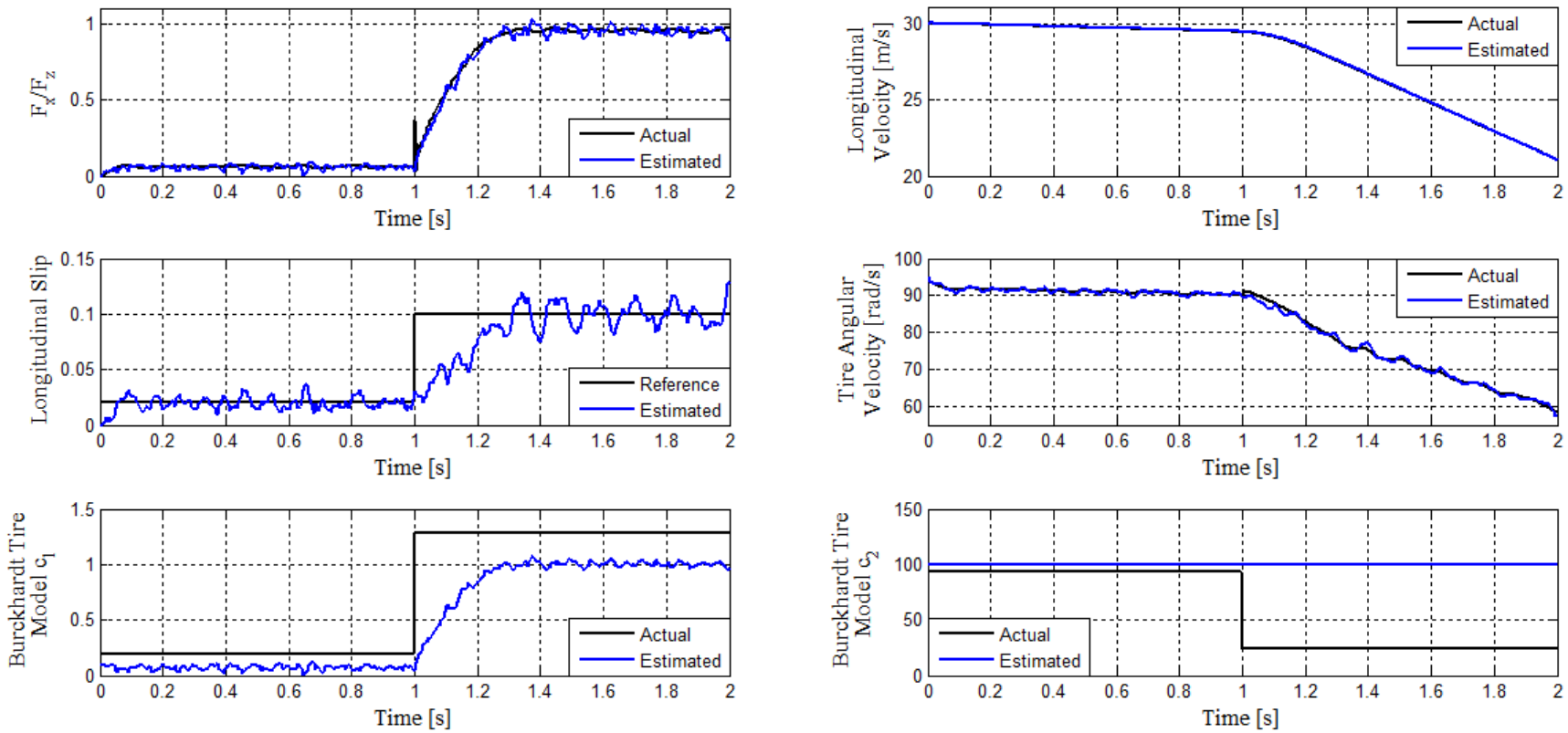
Figure 5.5. Wheel slip regulation simulation results during snow-dry road transitioning
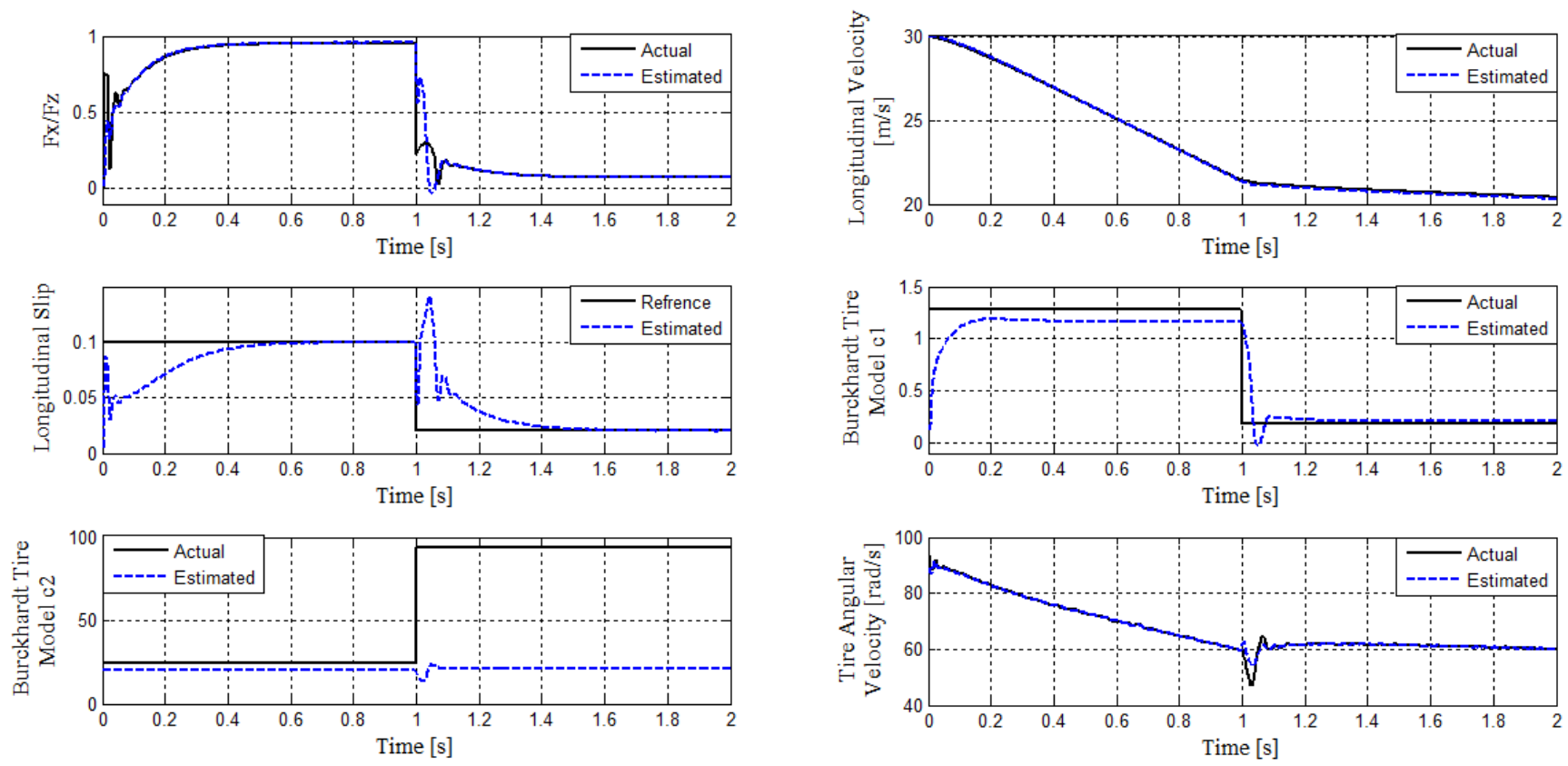
Figure 5.6. Wheel slip regulation simulation results during dry-snow road transitioning
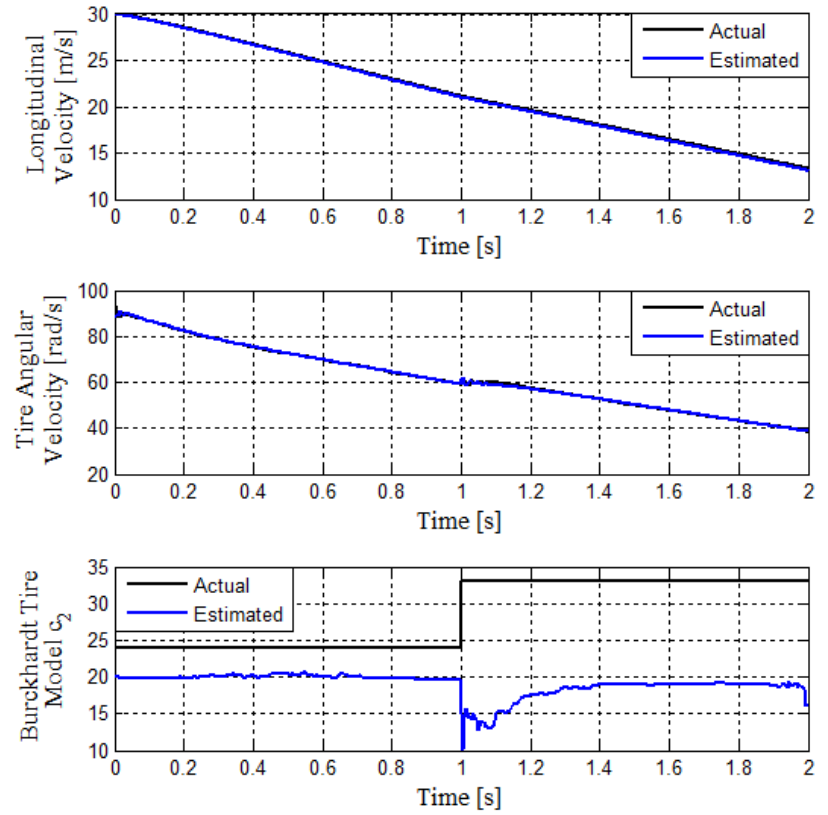
Figure 5.7. Wheel slip regulation simulation results during dry-wet road transitioning

Figure 5.8. Wheel slip regulation simulation results during dry-snow-wet road transitioning

5.4. Wheel Slip Regulation by Using DEKF with calculating λ^*

In this section, our aim is to design wheel slip regulator by using parameters, which are estimated by DEKF, to find peak value of F_x-λ figure(λ^*). Then λ^* is used as reference feedback to the system. The algorithm is shown in Figure 5.7.
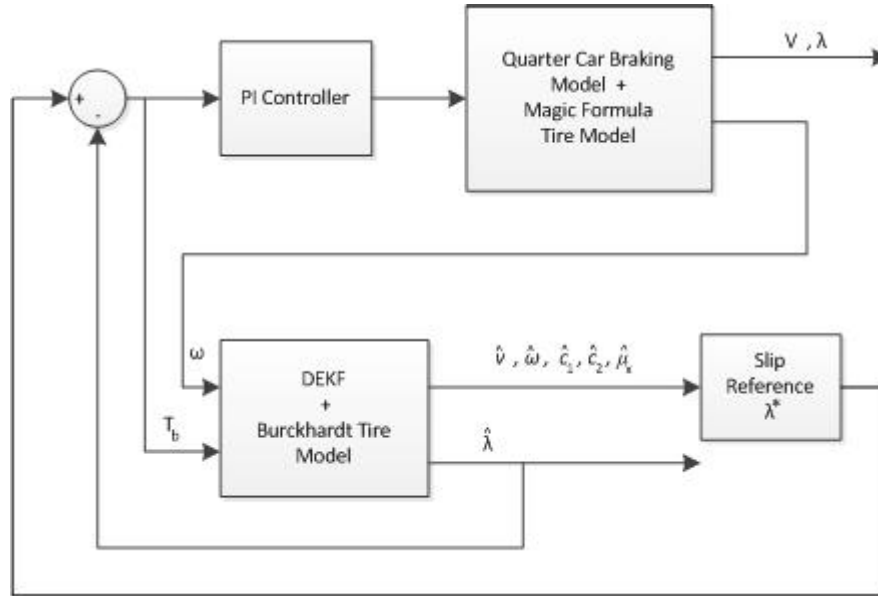
Figure 5.9. Block diagram for estimation of velocity and Burckhardt tire model parameters with calculating λ^*

As seen in Figure 5.10, after solving $\frac{dF_x}{d\lambda} = 0$, we can obtain λ^*, which selected as the F_x reached its maximum value, as shown in Eq. 5.9.

$$\lambda^* = -\frac{1}{c_2} \ln \frac{c_3}{c_1 c_2}$$

(5.9)
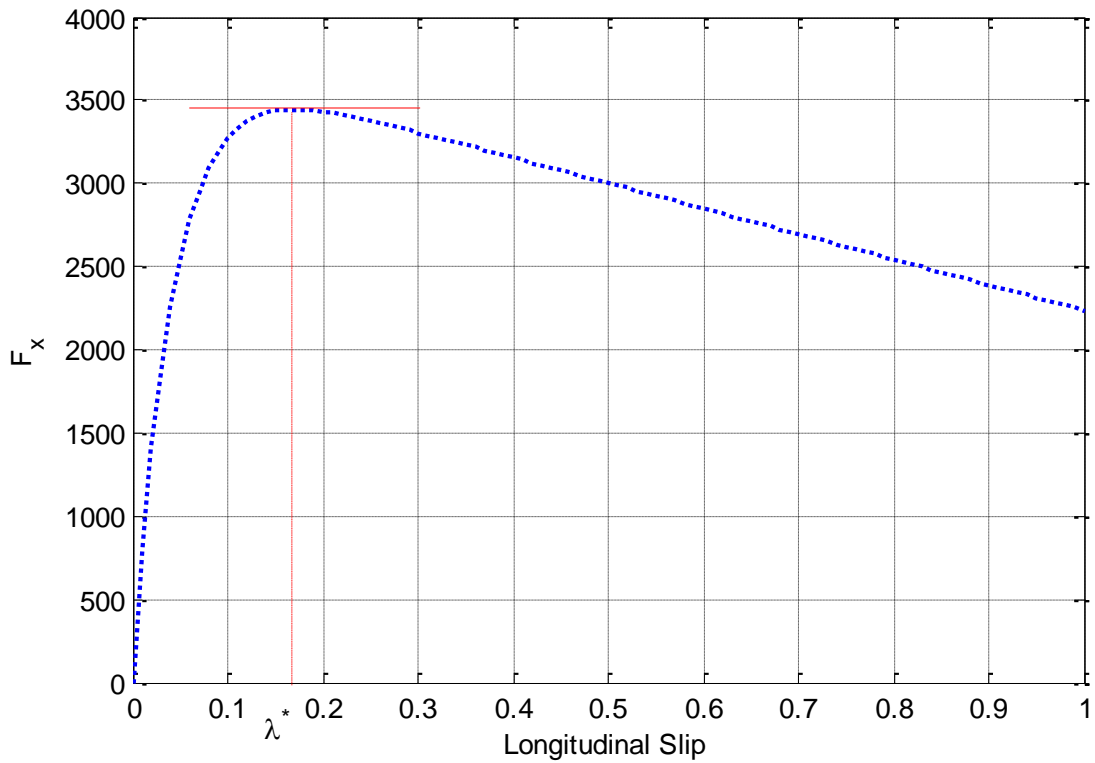
Figure 5.10. Ideal longitudinal slip for dry road

5.4.1 Simulation Results

As seen in figures below, estimation of longitudinal velocity and Burckhardt tire model parameters where ideal longitudinal tire slip is unknown are displayed. As evidenced by Figures 5.9, 5.10 and 5.11, longitudinal slip is tracking ideal longitudinal slip where both of which are estimated by EKF.
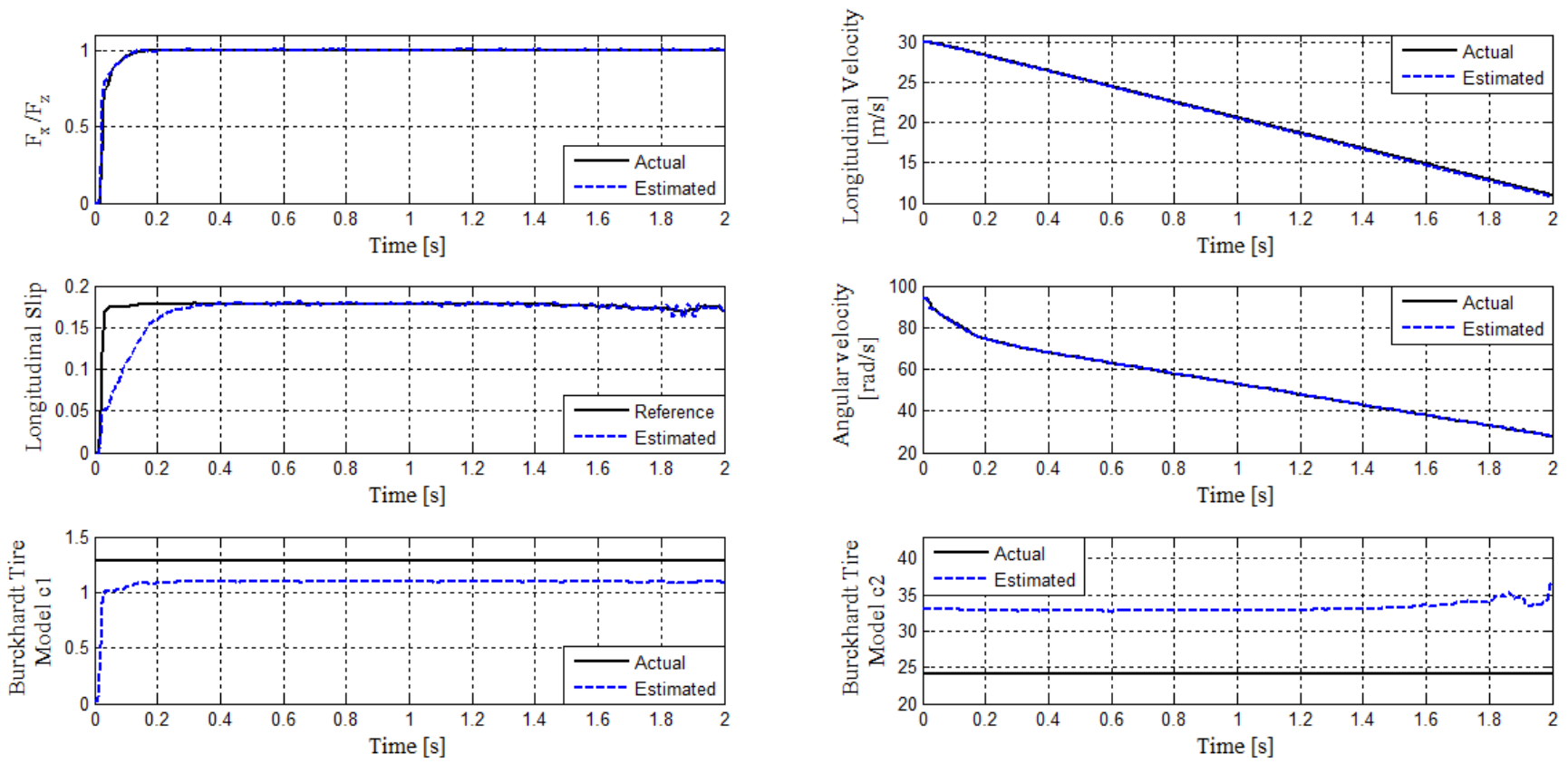
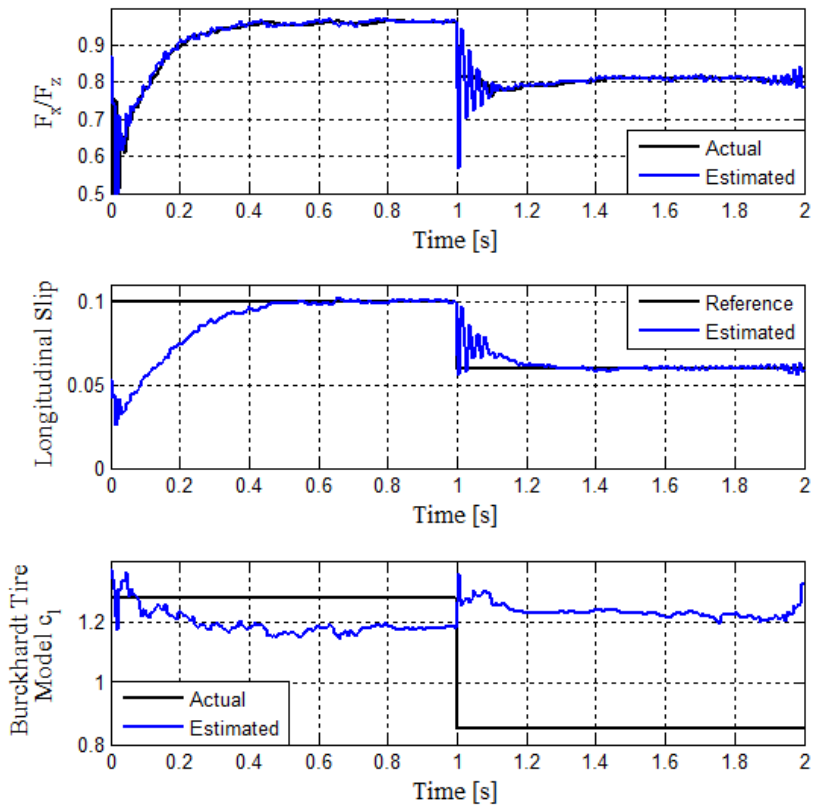Figure 5.11. Wheel slip regulation simulation results during dry road transitioning
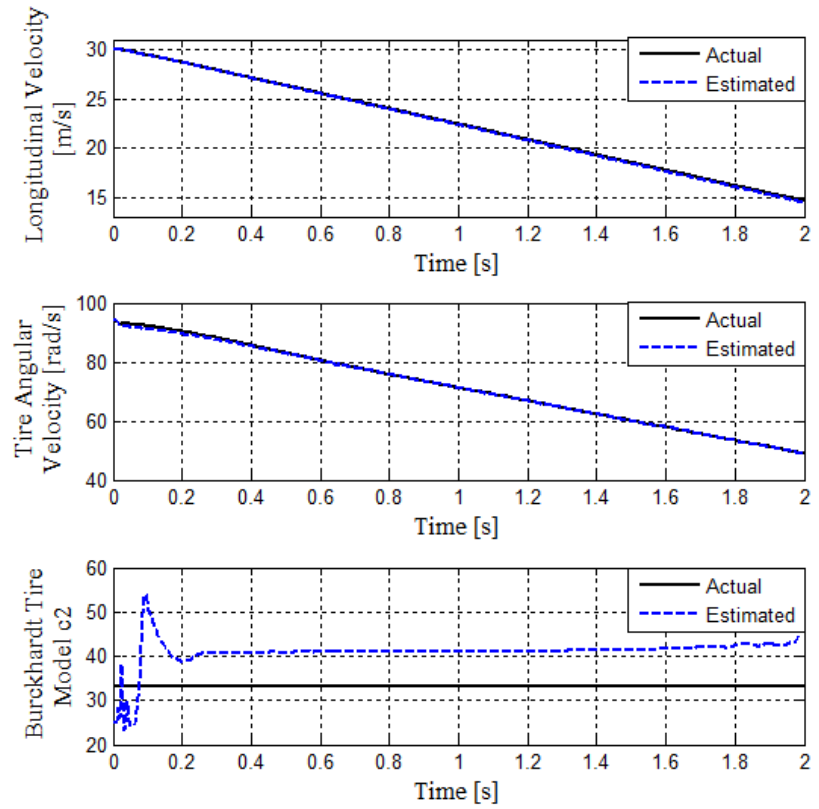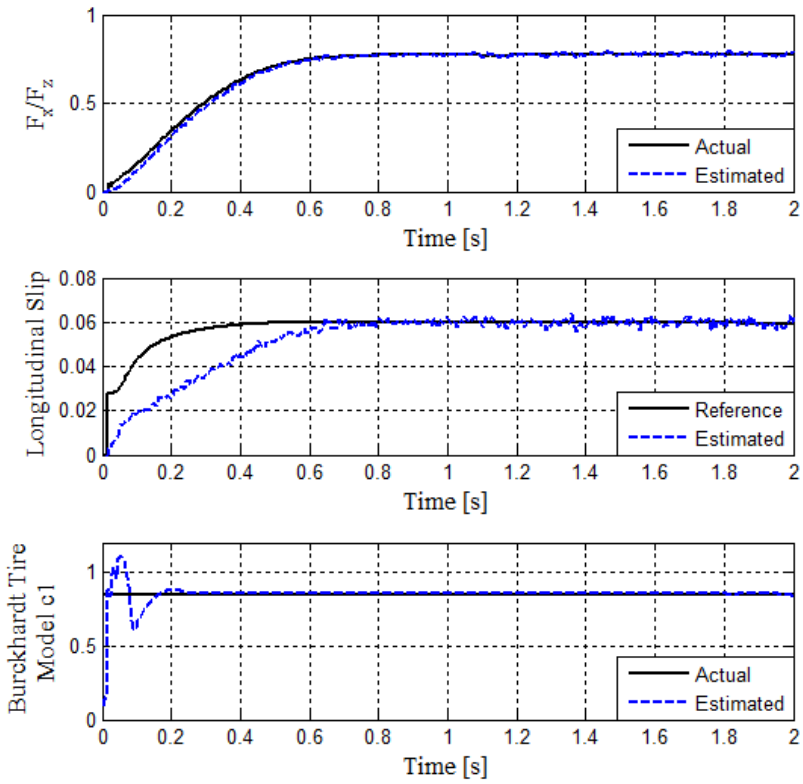
Figure 5.12. Wheel slip regulation simulation results during wet road transitioning

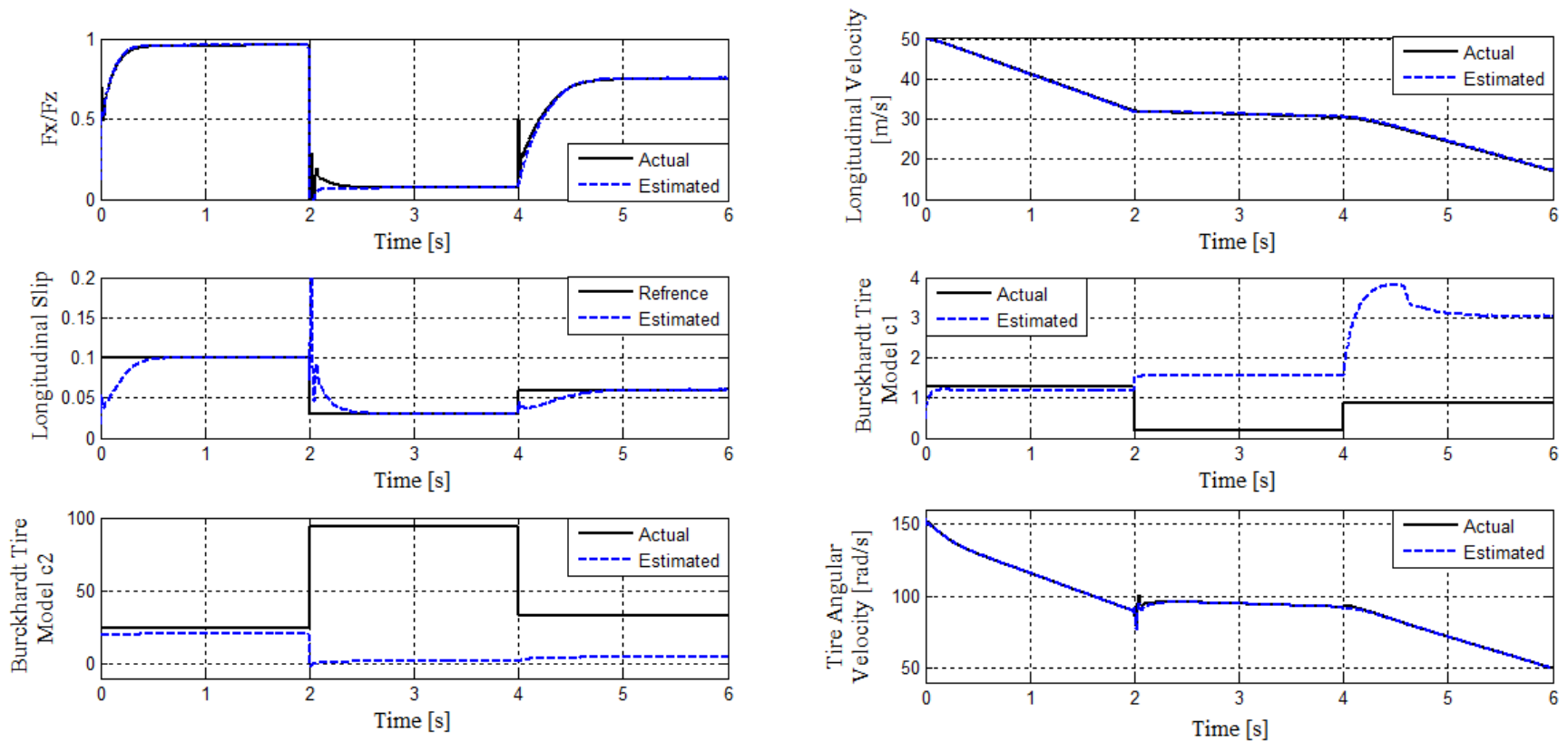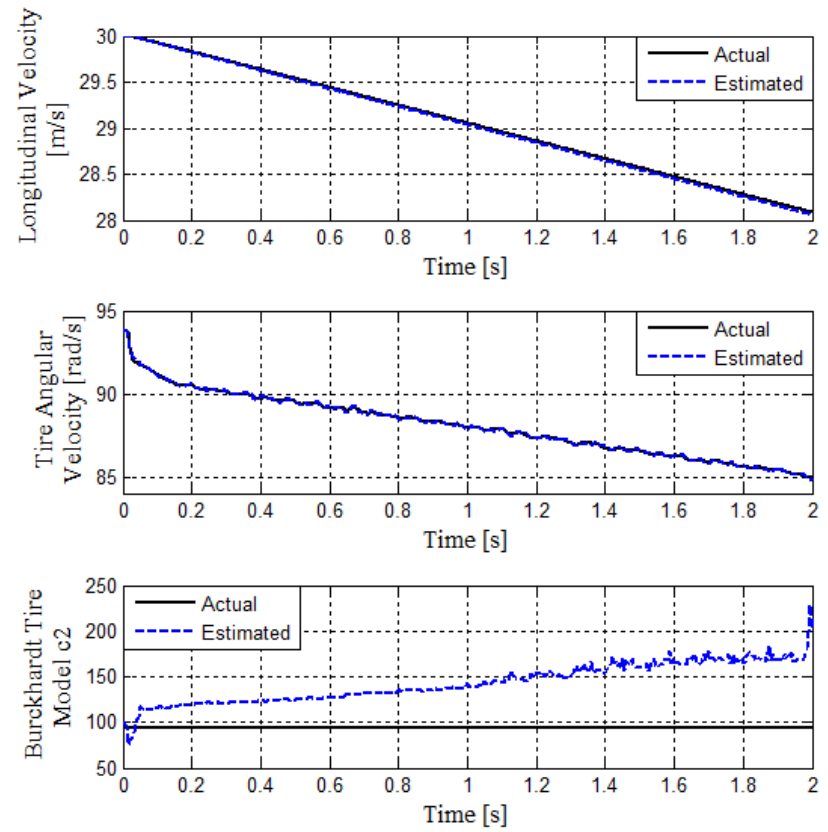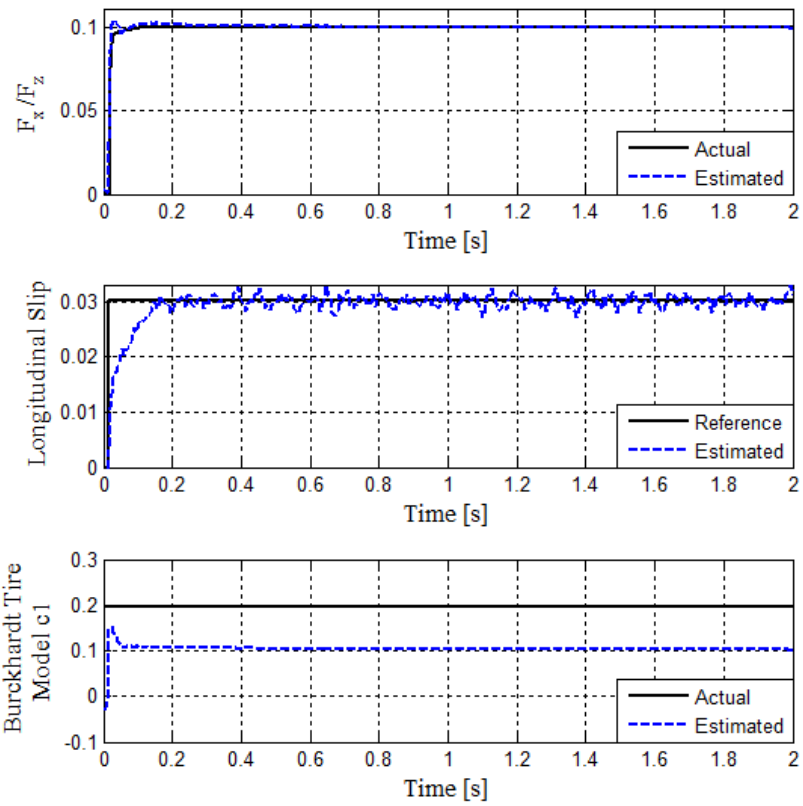Figure 5.13. Wheel slip regulation simulation results during snow road transitioning

Results are compared with the source model. As seen in figures estimation accuracy for longitudinal velocity, tire angular velocity and dynamic friction coefficient are high. Wheel slip is compared with perfect slip reference. The settling times for slip control in various roads are less. Estimation of c_1 and c_2 parameters of Burckhardt tire model are acceptable.

5.5. Conclusions

This chapter provided application of extended Kalman filter of quarter car braking model during longitudinal braking. Application of the Extended Kalman filter shows that accurate estimation of the absolute speed can be achieved even under significant braking skid on various road surfaces. Also, results show high accuracy slip tracking.

In addition, this chapter includes parameter of tire model identification by using EKF under various road conditions.

6. CONCLUSION AND FUTURE WORK

In this dissertation, estimators based on Kalman filtering are discussed. our aim is to estimate relevant vehicle states and parameters.

It starts with a discussion of a Kalman filter used for state estimation in a linear system. However, since the 'complete' vehicle system is nonlinear, the algorithm can not be applied directly and requires non-linear version of Kalman filter which is extended Kalman filter (EKF). The EKF can be viewed as an attempt to linearize a nonlinear system in some aspects such that a Kalman filter can be applied.

EKF is the most commonly used nonlinear estimator for state estimation in nonlinear system found in the literature. The algorithm linearizes a nonlinear system by using a first-order truncation of a Taylor series. It works well in case of the nonlinearity is not severe and the approximation error is small. However, if the nonlinearity is severe or the approximation error is not negligible, the degradation in estimation performance or even a divergence might occur.

The proposed system utilizes the measurements from source model. Extended Kalman filter observer was employed to aid in the estimation of vehicle body sideslip angle. The designed observer is adapted based on current vehicle state. As a result the observer uses the kinematic model-based estimate accurately during transient nonlinear maneuvers. The lateral force at each axle was estimated by observer based on measurements of yaw rate and lateral acceleration. Since lateral force generation may be reduced due to tire longitudinal forces from braking or drive traction, the lateral force potential of each axle was calculated in order to estimate the lateral force that would be generated in the absence of longitudinal forces.

A method of adaptive estimation was presented using dual extended Kalman filter (DEKF). This algorithm is used to estimate road friction coefficient and tire model parameters. The parameter identification approach was shown to accurately identify changes in these parameters during severe maneuver driving conditions.

Furthermore, extended Kalman filter is used to estimate true vehicle speed in quarter car braking model. Our aim is that wheel slip is tracking to perfect wheel slip in less time. The results show that wheel slip is well tracked.

In addition, the identification of friction coefficients and tire model parameters was shown to enable the control strategy to adapt to changes in various road transiting.

Results from the simulation demonstrated the ability of the method to predict the estimator accuracy.

In future extensions of this dissertation, Adaptive-tire will be used for online tuning of vehicle dynamics controllers.

APPENDIX

Table A.1. Burckhardt tire model constants in various road situations

Condition	c_1	c_2	c_3
Asphalt dry	1.28	23.99	0.52
Concrete dry	1.1973	25.168	0.5373
Asphalt wet	0.857	33.822	0.347
Snowy	0.1946	94.129	0.0646

Table A .2. Vehicle parameters for bicycle model

Parameter	Value (unit)	Parameter	Value (unit)
Mass (m)	1500 (kg)	Distance from front axle to CoG (l_f)	1 (m)
Front Tire Cornering Stiffness ($C_{\alpha f}$)	50000 (N/rad)	Distance from CoG to rear axle (l_r)	1 (m)
Rear Tire Cornering Stiffness ($C_{\alpha r}$)	45000 (N/rad)	Moment Inertia (I_z)	2500 (kgm^2)

Table A.3. Vehicle parameters for non-linear planar model

parameter	Value (unit)
Mass (m_v)	1987.9 (kg)
Distance from front to CoG (l_f)	1.1473 (m)
Distance from Cog to rear (l_r)	1.4307 (m)
Vehicle track (t)	1.48 (m)
Moment Inertia (I_z)	4510.25 (kgm^2)

Table A.4. Quarter car model parameters

Parameter	Value (unit)
Moment Inertia (J)	1 (kgm^2)
Wheel Radius (W_r)	0.32 (m)
Mass (m)	450 (Kg)

References

[1]   Peden, M., Scurfield, R., Sleet, D., Mohan, D., Hyder, A., Jarawan, E., and Mathers, C., World report on road traffic injury prevention, Technical report, World Health Organization, Geneva, **2004**.

[2]   Rajamani, R., Vehicle Dynamics and Control, Springer, **2006**.

[3]   Wong, J. Y., Theory of Ground Vehicles, John Wiley & Sons, INC, Third Edition, **2001**.

[4]   Electronic stability control coalition fact sheet, ESC Coalition and DEKRA Automotive Research, **2003**.

[5]   Aga, M., Okada, A., Analysis of vehicle stability control (VSC)＇s effectiveness from accident data, In Proceedings of the 18th International Technical Conference on the Enhanced Safety of Vehicles, number 541, **2003**.

[6]   Minh, N., B., Research On Sideslip Angle Estimation Using GPS and Multi-Rate Kalman Filter For Electric Vehicle Stability Control, Master of Engineering Thesis, University of Tokyo, **2012**.

[7] Ono, E., Asano, K., Sugai, M., Ito, S., Yamamoto, M., Sawada, M. et al., Estimation of automotive tire force characteristics using wheel velocity, *Control Engineering Practice*, 11, 1361–1370, **2003**.

[8] Ding, N., Taheri, S., Application of Recursive Least Square Algorithm on Estimation of Vehicle Sideslip Angle and Road Friction, *Hindawi Publishing Corporation Mathematical Problems in Engineering*, 10.1155/2010/541809, **2010**.

[9] Fukada, Y., Slip-angle estimation for vehicle stability control, *Vehicle System Dynamics*, 32, 375–388, **1999**.

[10] Hac, A., & Simpson, M. D., Estimation of vehicle side slip angle and yaw rate, In Proceedings of SAE world congress, Detroit, MI, **2000**.

[11] Gustafsson, F., Slip-based tire–road friction estimation, *Automatica*, 33(6), 1087–1099, **1997**.

[12] Ray, L. R., Nonlinear tire force estimation and road friction identification: Simulation and experiments, *Automatica*, 33(10), 1819–1833, **1997**.

[13] Suissa, A., Zomotor, Z., & Bottiger, F., Method for determining variables characterizing vehicle handling. US Patent 5,557,520, **1994**.

[14] Best, M. C., Gordon, T. J., & Dixon, P. J., An extended adaptive Kalman filter for real-time state estimation of vehicle handling dynamics. *Vehicle System Dynamics*, 34, 57–75, **2000**.

[15] Nishira, H., Kawabe, T., & Shin, S., Road friction estimation using adaptive observer with periodical modification, In Proceedings of the IEEE international conference on control and its applications, Kohala Coast, HI, **1999**.

[16] Canudas-de-Wit, C., Petersen, M. L., &Shiriaev A., A new nonlinear observer for tire/road distributed contact friction, In Proceedings of the42nd IEEE conference on decision and control, Maui, HI, **2003**.

 [17] Grip, H. F., Imsland, L., Johansen, T. A., Fossen, T. I., Kalkkuhl, J. C., &Suissa, A., Nonlinear vehicle velocity observer with road-tire friction adaptation, In Proceedings of the 45th IEEE conference on decisionand control, San Diego, CA, **2006**.

[18] Mancosu, F.,Speziari,D.,Ceresa,M.,&Sbarbati,P., A new methodology to get reliable input data for handling simulations, *Tire Science and Technology*, TSTCA, 27, 176–187, **1999**.

[19] Bolzern, P., Cheli, F., Falciola, G., Fresta, F., Estimation of the non-linear suspension tire cornering forces from experimental road test data, *Vehicle System Dynamics*, 31, 23–34, **1999**.

[20]   T. A. Wenzel, K. J. Burnham, M. V. Blundell & R. A. Williams, Dual extended Kalman filter for vehicle state and parameter estimation, *Vehicle System Dynamics: International Journal of Vehicle Mechanics and Mobility*, 44:2, 153-171, **2006**.

[21]   Gillespie, T.D., Fundamentals of Vehicle Dynamics, Warrendale: Society of Automotive Engineers (SAE), Inc, **1992**.

[22]   Ryu, J., State and Parameter Estimation For Vehicle Dynamics Control Using GPS, Doctor of Philosophy Thesis, Stanford University, **2004**.

[23]   Pacejka, H. B., Tyre and Vehicle Dynamics, Butterworth Heinemann, **2002**.

[24]   Burckhardt, M., ABS und ASR, Sicherheitsrelevantes, Radschlupf-Regel System, Lecture Scriptum, University of Braunschweig, Germany, **1987**.

[25]   Başlamışlı, S. Ç., Solmaz, S., Construction of a Rational Tire Model for High Fidelity Vehicle Dynamics Simulation under Extreme Driving and Environmental Conditions, Proceedings of ESDA2010 ASME 2010, 10th Biennial Conference on Engineering Systems Design and Analysis, Istanbul, Turkey, July, **2010**.

[26]   Kiencke, U., Nielsen, L., Automotive Control Systems for Engine, Driveline and Vehicle, Springer, **2000**.

[27]   Baslamisli, S., C., LPV Modeling and Robust Control of Yaw and Roll Modes of Road Vehicles, Doctor of Philosophy Thesis, Bogazici University, **2004**.

[28]   Wan, E. A., Nelson, A. T., Dual Extended Kalman Filter Methods, Kalman Filtering and Neural Networks, pp. 123-173: John Wiley & Sons, Inc, **2002**.

[29]   Kalman, R., R. Bucy, R., New results in linear filtering and prediction theory, ASME Journal of Basic Engineering, 83:95–108, **1961**.

[30]   Simon, D., Optimal state estimation: Kalman, H-infinity and nonlinear approaches, John Wiley and Sons, Inc., Hoboken, New Jersey, **2006**.

[31]   Best, M.C., Newton, A.P. and Tuplin, S., The identifying extended Kalman filter parametric system identification of a vehicle handling model, Proceedings of the Institution of Mechanical Engineers, Part K: Journal of Multi-body Dynamics, 221(1), pp. 87-98, **2007**.

[32]   Kobayashi, K., CheoP, K. C., Watanabe, K., Estimation of Absolute Vehicle Speed using Fuzzy Logic Rule-Based Kalman Filter, in Proc. of the American Control Conference Seattle, Washington,21-25 June **1995**.

[33]   Dorf, Richard C., Bishop, R., H., Modern Control Systems, 9th ed., Prentice–Hall Inc., New Jersey-07458, USA, 2001, Chapters 1, 5, pp. 1-23, pp. 173-206, **2001**.

[34]   http://en.wikipedia.org/wiki/PI_controller#PI_controller

CV

Credentials

First Name, Last Name: Arash, HOSSEINIAN AHANGARNEJAD

Place of Birth: Iran

Marital Status: Single

E-mail: arash.ahangarnejad@gmail.com

Adress: Hacettepe University, Beytepe Campus, Student Home, D Block, No.106, Ankara / Turkey

Education

High School: Meshkat, Tabriz, Iran.

B.S.: Islamic Azad University, Tabriz Branch.

Foreign Language: English.

Publication:

Adap-tire: EKF filtering for vehicle state estimation based on tire parameter adaptation.